# A remarkable troglomorphic ant, Yavnella laventa sp. nov. (Hymenoptera: Formicidae: Leptanillinae), identified as the first known worker of Yavnella Kugler by phylogenomic inference

Authors: Griebenow, Zachary Hayes, Isaia, Marco, and Moradmand, Majid

Source: Invertebrate Systematics, 36(12) : 1118-1138

Published By: CSIRO Publishing

URL: https://doi.org/10.1071/IS22035

The BioOne Digital Library (https://bioone.org/) provides worldwide distribution for more than 580 journals and eBooks from BioOne's community of over 150 nonprofit societies, research institutions, and university presses in the biological, ecological, and environmental sciences. The BioOne Digital Library encompasses the flagship aggregation BioOne Complete (https://bioone.org/subscribe), the BioOne Complete Archive (https://bioone.org/archive), and the BioOne eBooks program offerings ESA eBook Collection (https://bioone.org/esa-ebooks) and CSIRO Publishing BioSelect Collection (https://bioone.org/csiro-ebooks).

Your use of this PDF, the BioOne Digital Library, and all posted and associated content indicates your acceptance of BioOne's Terms of Use, available at www.bioone.org/terms-of-use.

Usage of BioOne Digital Library content is strictly limited to personal, educational, and non-commmercial use. Commercial inquiries or rights and permissions requests should be directed to the individual publisher as copyright holder.

BioOne is an innovative nonprofit that sees sustainable scholarly publishing as an inherently collaborative enterprise connecting authors, nonprofit publishers, academic institutions, research libraries, and research funders in the common goal of maximizing access to critical research.

Downloaded From: https://complete.bioone.org/journals/Invertebrate-Systematics on 13 Jun 2025
Terms of Use: https://complete.bioone.org/terms-of-use

RESEARCH PAPER
https://doi.org/10.1071/IS22035

Invertebrate Systematics

# A remarkable troglomorphic ant, *Yavnella laventa* sp. nov. (Hymenoptera: Formicidae: Leptanillinae), identified as the first known worker of *Yavnella* Kugler by phylogenomic inference

Zachary Hayes Griebenow[A,*], Marco Isaia[B] and Majid Moradmand[C]

For full list of author affiliations and declarations see end of paper

***Correspondence to:**
Zachary Hayes Griebenow
Department of Entomology and Nematology, University of California, Davis, CA, USA
Email: zgriebenow@ucdavis.edu

**Handling Editor:**
Prashant Sharma

**Received:** 21 July 2022
**Accepted:** 27 October 2022
**Published:** 5 December 2022

**Cite this:**
Griebenow ZH *et al.* (2022)
*Invertebrate Systematics*
**36**(12), 1118–1138. doi:10.1071/IS22035

## ABSTRACT

The ant subfamily Leptanillinae (Hymenoptera: Formicidae) consists of minute soil-dwelling species, with several genera within this clade being based solely upon males, including *Yavnella* Kugler. The dissociation of males and workers has resulted in taxonomic confusion for the Leptanillinae. We here describe the worker caste of *Yavnella*, facilitated by maximum-likelihood and Bayesian inference from 473 partitioned ultra-conserved element loci, this dataset including 49 other leptanilline species, both described and undescribed. *Yavnella laventa* **sp. nov.** is described from seven worker specimens collected in south-western Iran from the *Milieu Souterrain Superficiel*, a subterranean microhabitat consisting of air-filled cavities among rock and soil fragments, which is subject to similar environmental conditions as caves. This species has bizarrely elongated appendages, which suggests that it is confined to cavities, in contrast with the soil-dwelling behaviour observed in other leptanilline ants. Based on its gracile phenotype relative to other Leptanillinae, *Y. laventa* shows remarkable adaptations for subterranean life, making it one of a very few examples of this syndrome among the ants. Moreover, the discovery of the worker caste of *Yavnella* expands our morphological knowledge of the leptanilline ants. We provide worker- and male-based diagnoses of *Yavnella*, along with a key to the genera of the Leptanillinae for which workers are known. The worker caste of *Yavnella* as known from this species is immediately recognisable, but the possibility must be noted that described workers of *Leptanilla* may in fact belong to *Yavnella*. Further molecular sampling is required to test this hypothesis.

ZooBank: urn:lsid:zoobank.org:pub:A54A5766-F35A-4074-9353-1C70FE3955D3

**Keywords:** Insecta, Iran, *Milieu Souterrain Superficiel*, molecular systematics, Palaearctic, phylogenomics, subterranean biology, troglomorphism.

## Introduction

The Leptanillinae (Hymenoptera: Formicidae) are a group of miniscule, cryptic ants, found in many tropical and warm temperate areas of the Old World. Workers are completely blind and exclusively soil dwelling. The biology of only a few leptanillines has been studied – these are specialised predators of geophilomorph centipedes (Masuko 1990; Hsu *et al.* 2017) or of forcepstails (Diplura: Japygidae) (Ito *et al.* 2022). The subfamily is divided into two monophyletic tribes, Leptanillini and Anomalomyrmini (Bolton 1990; Borowiec *et al.* 2019), with the monotypic genus *Opamyrma* unplaced to tribe (Ward and Fisher 2016). Of the tribe Leptanillini, in only *Leptanilla* Emery, 1870 are the worker and queen known, with the remaining three genera – *Scyphodon* Brues, 1925; *Noonilla* Petersen, 1968; and *Yavnella* Kugler, 1987 – known only from male specimens. So far as is known, queens of *Leptanilla* are wingless and blind, resembling miniature versions of the dichthadiigynes observed in army ants of the subfamily Dorylinae (Hölldobler and Wilson 1990; Ito and Yamane 2020), whereas queens in the Anomalomyrmini are alate (Bolton 1990; Baroni Urbani and de Andrade 2006) or ergatoid (Billen *et al.* 2013).

Conversely, males of Leptanillinae are always fully winged. Owing to collecting bias towards males, three genera in the tribe Leptanillini have been described solely from male specimens, as have some species of *Leptanilla*. Further, there is a large diversity of undescribed male morphospecies in the subfamily (Griebenow 2021). The Leptanillinae are therefore afflicted by parallel taxonomy. Out of more than 60 described species, the sexes have been associated only in *Leptanilla japonica* Baroni Urbani, 1977 (Ogata *et al.* 1995), *Opamyrma hungvuong* Yamane, Bui & Eguchi, 2008 (Yamada *et al.* 2020) and *Protanilla lini* Terayama, 2009 (Griebenow 2020). Males were collected from the same nests as corresponding workers only in *L. japonica* and *O. hungvuong*, with the male of *P. lini* being indirectly identified using phylogenomic inference.

*Yavnella* is the most recently described of the male-based leptanilline genera, established by Kugler (1986) for two species from Israel and Kerala (India), by original designation. The phylogenetic analyses of Griebenow (2020, 2021) included a variety of undescribed male *Yavnella* morphospecies along with *Yavnella argamani* Kugler, 1987 and recovered the genus as monophyletic with high support, irrespective of data or inferential framework. The genus is most diverse in mainland South-east Asia (this diversity remaining entirely undescribed), with additional representatives in the Indian subcontinent and the Arabian subcontinent as far south as Yemen (Collingwood and Agosti 1996). Borowiec *et al.* (2019) also robustly recovered this clade, under a sampling regime overlapping with Griebenow (2020, 2021), although Borowiec *et al.* (2019) did not explicitly identify this clade as *Yavnella*.

Here, we describe *Yavnella laventa* **sp. nov.** from Fārs Province, Iran, based on seven worker specimens, collected in the *Milieu Souterrain Superficiel* (MSS) at depths of 0.6–1 m within a debris flow adjacent to a salt cave entrance. According to Uéno (1980) and Culver and Pipan (2014), the MSS is a subterranean network of empty air-filled cracks and voids. *Yavnella laventa* is here identified as belonging to *Yavnella* based upon phylogenomic inference from ultraconserved elements (UCEs) and constitutes the first known representatives of the worker caste in that genus. The phenotype of *Y. laventa* is strikingly different from that of all other known leptanilline workers, with the mandibles, antennae and legs being elongated in what are apparently examples of strong adaptation to subterranean habitats, i.e. troglomorphism. With the discovery of the worker caste of *Yavnella* we provide a revised worker-based key to the genera of the Leptanillinae, with figures.

A natural classification of the Leptanillinae is made difficult by dissociation of the dissimilar worker and male forms of leptanilline ants, which results in parallel taxonomy. Therefore, the identification of the worker caste of *Yavnella*, a major leptanilline clade heretofore known only from male specimens, begins to correct this parallel taxonomy. The phylogenomic approach by which *Y. laventa* was identified as *Yavnella*, despite the lack of known conspecific male specimens with which to determine the generic identity of this species, affirms the utility of molecular data in connecting unassociated and drastically divergent forms in polymorphic organisms.

From an ecological perspective, the troglomorphism exhibited by *Y. laventa* is remarkable in the context of the Formicidae as a whole. After *Leptogenys khammouanensis* Roncin & Deharveng, 2003 (Ponerinae: Ponerini) and *Aphaenogaster gamagumayaa* Naka & Maruyama, 2018 (Myrmicinae: Stenammini), *Y. laventa* is only the third arguably troglomorphic ant species described (Roncin and Deharveng 2003; Naka and Maruyama 2018) out of >15 000 described species. In contrast to *L. khammouanensis* and *A. gamagumayaa*, *Y. laventa* was not collected in an underground space between rocks accessible to humans (i.e. a 'cave'), but in the network of subterranean fissures and voids that constitutes the MSS, which is known to harbour species with troglomorphic traits (see Mammola *et al.* 2016 for a comprehensive review on the topic).

## Materials and methods

### Materials

In total, 63 specimens belonging to the Leptanillinae were included in this study, in addition to *Martialis heureka* Rabeling & Verhaagh, 2008 (Martialinae) as an outgroup. Ultra-conserved element data are included in this study for 51 taxa of those 63, including *M. heureka*, a representative of *Y. laventa* (CASENT0842745), along with representatives of all major subclades of that subfamily. Thirteen of these specimens are newly sequenced in this study. Twelve specimens of *Protanilla* Taylor in Bolton (1990) and *Leptanilla* along with one *Anomalomyrma* Taylor in Bolton (1990) were morphologically examined, but not sequenced (Table 1). Generic assignment of sequenced material follows Griebenow (2020) rather than Borowiec *et al.* (2019) where sampling overlaps with those studies. Additional collection data for these specimens are provided in a Supplementary Table S1.

Specimens are deposited at the following institutions (abbreviations follow http://hbs.bishopmuseum.org/codens/, where applicable): the California Academy of Sciences, San Francisco, USA (CAS); the California State Collection of Arthropods, Sacramento, CA, USA (CSCA); the Biodiversity Museum, University of Hong Kong, Hong Kong, PR China (HKUBM); the Jalal Afshar Zoological Museum, Department of Plant Protection, College of Agriculture and Natural Resources, University of Tehran, Karaj, Iran (JAZM); the Museum of Comparative Zoology, Harvard University, Cambridge, MA, USA (MCZC); Lund University, Lund, Sweden (MZLU); National Changhua University of Education, Changhua, Taiwan (NCUE); the Okinawa Institute of Science & Technology, Onna-son, Japan (OIST); the Royal Ontario Museum, Toronto, ON, Canada (ROME); the R. M. Bohart Museum of Entomology, University of California, Davis, CA, USA (UCDC); the Museum für Naturkunde der

**Table 1.** Specimens used in this study, with summary statistics pertaining to the 313 498-bp alignment in the cases of those specimens for which ultra-conserved elements (UCEs) were enriched using the *hym-v2* probe set of Branstetter *et al.* (2017).

| Taxon name | Caste or sex | Extraction code | Specimen identifier | SRA | Percentage missing | – | ? | Specimen physically examined |
|---|---|---|---|---|---|---|---|---|
| *Anomalomyrma boltoni* | ☿ | D0953 | CASENT0217032 | SRR11742957 | 9.617 | 23 959 | 6191 | No |
| *Anomalomyrma* indet. | ♀ | – | CASENT0178553 | – | – | – | – | Yes |
| *Leptanilla boltoni*[A] | ☿ | – | CASENT0260440 | – | – | – | – | Yes |
| *Leptanilla boltoni*[B] | ☿ | D2139 | CASENT0842753 | SRR16605703 | 30.154 | 83 505 | 11 027 | Yes |
| *Leptanilla* cf. *zaballosi*[B] | ♂ | D1865 | CASENT0842630 | SRR16814131 | 4.165 | 7773 | 5284 | Yes |
| *Leptanilla charonea*[B] | ☿ | D1860 | CASENT0842648 | SRR16814135 | 25.538 | 8457 | 71 603 | Yes |
| *Leptanilla* GR01 | ♂ | D0969 | CASENT0106236 | SRR11881502 | 7.294 | 13 496 | 9371 | Yes |
| *Leptanilla* GR02 | ♂ | D0967 | CASENT0106060 | SRR11881501 | 49.008 | 8628 | 14 5011 | Yes |
| *Leptanilla* GR03 | ♂ | D0965 | CASENT0106058 | SRR11793843 | 17.53 | 49 943 | 5014 | Yes |
| *Leptanilla havilandi*[A] | ☿ | – | CASENT0010809 | – | – | – | – | Yes |
| *Leptanilla* KE01[A] | ☿ | – | CASENT0842721 | – | – | – | – | Yes |
| *Leptanilla revelierii* | ☿ | D1866 | CASENT0842627 | SRR11881510 | 5.992 | 5767 | 13 017 | Yes |
| *Leptanilla thai*[A] | ☿ | – | CASENT0842784 | – | – | – | – | Yes |
| *Leptanilla theryi*[A] | ☿ | – | CASENT0842751 | – | – | – | – | Yes |
| *Leptanilla* TH01 | ♂ | D0679 | CASENT0119792 | SRR11881509 | 3.229 | 8026 | 2098 | Yes |
| *Leptanilla* TH07[B] | ♂ | D1051 | CASENT0227554 | SRR16814133 | 6.877 | 8864 | 12 696 | No |
| *Leptanilla* zhg-au01 | ♂ | D1544 | CASENT0758873 | SRR11793860 | 40.17 | 105 500 | 20 431 | Yes |
| *Leptanilla* zhg-au02 | ♂ | D1545 | CASENT0758864 | SRR11793848 | 31.835 | 90 684 | 9119 | Yes |
| *Leptanilla* zhg-au07[B] | ♂ | D1716 | CASENT0758869 | SRR11793844 | 12.454 | 25 456 | 13 587 | Yes |
| *Leptanilla* zhg-bt01 | ♂ | D1682 | CASENT0842617 | SRR11793849 | 25.583 | 63 488 | 16 714 | Yes |
| *Leptanilla* zhg-bt02[B] | ♂ | D2137 | CASENT0842612 | SRR16605702 | 8.374 | 16 088 | 10 165 | Yes |
| Leptanilla zhg-es01[B] | ♂ | D1864 | CASENT0842633 | SRR16814129 | 93.426 | 38 402 | 25 4486 | Yes |
| *Leptanilla* zhg-id01 | ♂ | D1754 | CASENT0842626 | SRR11881505 | 53.68 | 138 317 | 29 970 | Yes |
| *Leptanilla* zhg-id02[B] | ♂ | D2140 | CASENT0106358 | SRR16605701 | 9.388 | 15 548 | 13 884 | Yes |
| *Leptanilla* zhg-my02 | ♂ | D1683 | CASENT0106451 | SRR11793840 | 46.237 | 121 625 | 23 326 | Yes |
| *Leptanilla* zhg-my03 | ♂ | D1686 | CASENT0842618 | SRR11793851 | 10.706 | 27 395 | 6167 | Yes |
| *Leptanilla* zhg-my04 | ♂ | D1684 | CASENT0842553 | SRR11793838 | 24.507 | 67 573 | 9255 | Yes |
| *Leptanilla* zhg-my05 | ♂ | D1685 | CASENT0842568 | SRR11793837 | 36.562 | 100 676 | 13 946 | Yes |
| *Leptanilla* zhg-th01 | ♂ | D1679 | CASENT0842614 | SRR11793854 | 22.33 | 62 139 | 7865 | Yes |
| *Martialis heureka* | ☿ | D0751 | CASENT0106181 | SRR11881511 | 26.078 | 77 626 | 4127 | No |
| *Noonilla* zhg-my01 | ♂ | D1690 | CASENT0842585 | SRR11793857 | 68.09 | 137 042 | 76 418 | Yes |
| *Noonilla* zhg-my02 | ♂ | D1691 | CASENT0842599 | SRR11793856 | 41.309 | 110 602 | 18 900 | Yes |
| *Noonilla* zhg-my04 | ♂ | D1694 | CASENT0842610 | SRR11793855 | 62.12 | 143 346 | 51 399 | Yes |
| *Noonilla* zhg-my06 | ♂ | D1688 | CASENT0106373 | SRR11793842 | 19.739 | 56 504 | 5376 | Yes |
| *Opamyrma hungvuong* | ☿ | D0734 | CASENT0178347 | SRR11742960 | 30.055 | 86 938 | 7285 | No |
| *Protanilla beijingensis*[A] | ☿ | – | CASENT0842639 | – | – | – | – | Yes |
| *Protanilla* indet.[A] | ♀ | – | CASENT0106383 | – | – | – | – | Yes |
| *Protanilla izanagi*[A] | ☿ | – | CASENT0842850 | – | – | – | – | Yes |

(*Continued on next page*)

**Table 1.** (*Continued*)

| Taxon name | Caste or sex | Extraction code | Specimen identifier | SRA | Percentage missing | – | ? | Specimen physically examined |
|---|---|---|---|---|---|---|---|---|
| *Protanilla jongi*[A] | ☿ | – | CASENT0824693 | – | – | – | – | Yes |
| *Protanilla lini* | ☿ | D0381 | CASENT0007002 | SRR11742961 | 8.892 | 25 437 | 2438 | No |
| *Protanilla lini* | ☿ | D1756 | OKENT0018456 | SRR11881504 | 4.621 | 12 704 | 1783 | Yes |
| *Protanilla* TH01 | ♂ | D0678 | CASENT0119776 | SRR12006305 | 7.425 | 11 231 | 12 045 | Yes |
| *Protanilla* TH03 | ♂ | D0807 | CASENT0119791 | SRR11742954 | 11.162 | 23 876 | 11 116 | Yes |
| *Protanilla* psw-my01[A] | ☿ | – | CASENT0842640 | – | – | – | – | Yes |
| *Protanilla* VN03 | ☿ | D0896 | CASENT0179565 | SRR11742951 | 9.845 | 25 634 | 5231 | Yes |
| *Protanilla wallacei*[A,C] | ☿ | – | CASENT0842699 | – | – | – | – | Yes |
| *Protanilla wardi*[B] | ☿ | D2138 | CASENT0221924 | SRR16605700 | 10.736 | 22 387 | 11 271 | Yes |
| *Protanilla* zhg-my01[B] | ♂ | D2166 | CASENT0842730 | SRR19638225 | 52.837 | 15 267 | 150 377 | Yes |
| *Protanilla* zhg-vn01 | ♂ | D1678 | CASENT0842613 | SRR11793859 | 37.799 | 98 707 | 19 792 | Yes |
| *Yavnella argamani* | ♂ | D1081 | CASENT0235253 | SRR11793861 | 9.901 | 25 943 | 5096 | Yes |
| *Yavnella* indet.[B] | ♂ | D1914 | CASENT0842660 | SRR16605699 | 4.585 | 7279 | 7095 | Yes |
| *Yavnella laventa*[B] | ☿ | D2170 | CASENT0842745 | SRR19638603 | 16.513 | 23 786 | 27 981 | Yes |
| *Yavnella* MM01 | ♂ | D0876 | CASENT0179537 | SRR11742953 | 18.204 | 51 880 | 5189 | Yes |
| *Yavnella* nr. *indica* | ♂ | D1689 | CASENT0106375 | SRR11793841 | 35.874 | 107 333 | 5132 | Yes |
| *Yavnella* TH02 | ♂ | D0677 | CASENT0119531 | SRR11881508 | 4.243 | 4402 | 8900 | Yes |
| *Yavnella* TH03 | ♂ | D0800 | CASENT0129721 | SRR11742956 | 8.304 | 20 458 | 5575 | Yes |
| *Yavnella* TH04 | ♂ | D0801 | CASENT0129695 | SRR11742958 | 8.848 | 20 176 | 7562 | Yes |
| *Yavnella* TH06 | ♂ | D0803 | CASENT0129609 | SRR11742955 | 9.72 | 20 953 | 9520 | Yes |
| *Yavnella* TH08 | ♂ | D1052 | CASENT0227775 | SRR11881506 | 6.084 | 4569 | 14 504 | Yes |
| *Yavnella* zhg-bt01 | ♂ | D1681 | CASENT0842616 | SRR11793850 | 15.934 | 22 811 | 27 141 | Yes |
| *Yavnella* zhg-th01 | ♂ | D1680 | CASENT0842615 | SRR11793853 | 8.834 | 19 229 | 8464 | Yes |
| *Yavnella* zhg-th03[B] | ♂ | D2169 | CASENT0842750 | SRR19638284 | 60.123 | 2714 | 185 771 | Yes |
| *Yavnella* zhg-th04[B] | ♂ | D1906 | CASENT0842657 | SRR16605698 | 11.324 | 9172 | 26 327 | Yes |

[A] Not sequenced.
[B] Sequences new to this study.
[C] *Nomen nudum*.

Humboldt-Universität, Berlin, Germany (ZMHB); and the Zoological Museum, University of Isfahan, Isfahan, Iran (ZMUI).

## Collection and specimen preparation

Specimens of *Yavnella laventa* **sp. nov.** were collected using subterranean sampling devices, i.e. two buried pitfall traps, placed in the MSS. The buried pitfall traps (hereinafter 'MSS traps') consisted of a rigid plastic cup, with holes bored in them midway from top to bottom to prevent flooding, and a horizontal stone placed on top. These were set in a clast on the bank of a wadi, opposite to a salt diapir (Fig. 1) (the Khoorab Salt Dome; Abbassi *et al.* 2015). These MSS traps were placed by slope boring at depths of 60–100 cm, baited with sardines and dates jointly contained in small vials, and half filled with brine. We attempted to measure relative humidity (RH) within the MSS using a Lascar EL-USB-2 data logger buried adjacent to the MSS traps. Brine is not an ideal preservative for purposes of acquiring DNA, but was used in a broad survey of salt karst fauna in the vicinity of Khoorab because of low evaporative rate. Although extraction of a genome-scale molecular dataset was successful when attempted with a single specimen (see 'Sequencing & data processing'), we recommend that future targeted efforts to collect leptanilline ants in the MSS or in salt caves use ethanol as a preservative, with traps being set for much briefer periods than outlined below.

Traps were left for 15 months, from 14 February 2019 to 26 June 2020, at the end of which specimens were

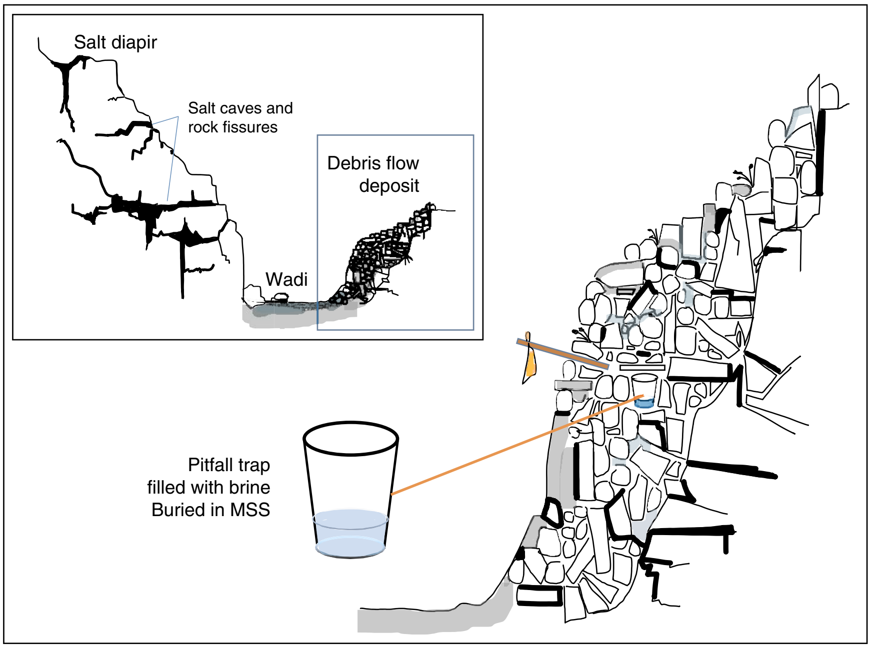

**Fig. 1.** Layout of MSS traps, and position relative to the adjacent salt diapir (the Khoorab Salt Dome) in which Last Cave is located.

transferred to 80 or 95% ethanol, the latter if intended for non-destructive DNA extraction. A few specimens remained in brine and were used for dissection and imaging. In addition, four pitfall traps baited in the same way and containing the same liquid were placed at ground level inside an adjacent salt cave ('Last Cave') within the Khoorab Salt Dome, for the same duration as the MSS traps, but no *Y. laventa* were collected in these traps. We measured RH within Last Cave using the same data loggers as listed above.

## Sequencing & data processing

For the specimens newly sequenced for this study, DNA was extracted non-destructively using a Dneasy Blood & Tissue Kit (Qiagen Inc., Valencia, CA, USA) with $H_2O$ at room temperature to elute DNA, or, in the case of CASENT0842745 and several other samples, 56°C buffer AE (Cruaud *et al.* 2019) in order to increase DNA yield. Genomic concentrations were quantified for each sample with a Qubit fluorometer (ver. 2.0, Life Technologies Inc., Carlsbad, CA, USA). Input DNA was sheared using a Diagenode Bioruptor (Diagenode, Denville, NJ, USA) or Qsonica Q800R3-110 (Qsonica Inc., Newtown, CT, USA). Sheared product was used as input for the modified library preparation protocol of Branstetter *et al.* (2017), with the ant-specific version of the UCE probe set *hym-v2* (Branstetter *et al.* 2017). Enrichment success and size-adjusted DNA concentrations of pooled libraries were assessed using the SYBR FAST qPCR kit (Kapa Biosystems, Wilmington, MA, USA), and all pools were combined into an equimolar final pool. Final pools were sequenced on an Illumina HiSeq X at Novogene (Sacramento, CA, USA) or prepared, enriched and sequenced using similar protocols at RAPiD Genomics (Gainesville, FL, USA). Refer to Ward and Blaimer (2022) for further details on library preparation and enrichment. For sequencing protocols implemented for the phylogenomic data used in this study that have been previously published, refer to Griebenow (2020).

The FASTQ output was demultiplexed and cleansed of adapter contamination and low-quality reads using *illumiprocessor* (ver. 2.1, B. C. Faircloth, see https://github.com/faircloth-lab/illumiprocessor) in the PHYLUCE bioinformatic software package (ver. 1.7.1, see https://phyluce.readthedocs.io/en/latest/; Faircloth 2016). Raw reads were assembled with SPAdes (ver. 3.12.0, see https://github.com/ablab/spades; Bankevich *et al.* 2012). Species-specific contig assemblies were obtained with the ant-specific *hym-v2* probe set (Branstetter *et al.* 2017), aligned with MAFFT L-INS-I (ver. 7.741, see https://github.com/GSLBiotech/mafft; Katoh and Toh 2010), and trimmed with Gblocks (ver. 0.91, see https://home.cc.umanitoba.ca/~psgendb/doc/Castresana/Gblocks_documentation.html; Castresana 2000) within a PHYLUCE workflow modified from Faircloth (2016) with min_identity = 80 within *phyluce_assembly_match_contigs_to_probes.py*, resulting in an alignment 313 498 bp long. This alignment was 76.79% complete, composed of 39.1% parsimony-informative sites; AT content was 57.4%. Summary statistics for this alignment were computed with the *summary* command in AMAS (see https://github.com/marekborowiec/AMAS; Borowiec 2016) (Table 1).

## Phylogenomic inference

Partitioning to generate subsets of each UCE locus was performed using PartitionUCE (see https://github.com/Tagliacollo/PartitionUCE; Tagliacollo and Lanfear 2018). Using IQ-Tree (ver. 2.1.2, see http://www.iqtree.org/;

Minh *et al.* 2020) on the CIPRES Science Gateway (ver. 3.3, see http://www.phylo.org/; Miller *et al.* 2010), partition schemes were inferred with ModelFinder in IQ-Tree (ver. 2.1.2; Kalyaanamoorthy *et al.* 2017) using subsets generated by PartitionUCE for the complete alignment, with the Bayesian Information Criterion (BIC) deciding among available partitioning schemes, followed by maximum-likelihood (ML) phylogenetic inference under these partition schemes (Chernomor *et al.* 2016) for 1000 ultrafast bootstraps (UFBoot) (Hoang *et al.* 2018) and SH-like approximate likelihood ratio test (SH-aLRT) (Guindon *et al.* 2010) replicates. The relaxed hierarchical clustering algorithm was implemented in these analyses (Lanfear *et al.* 2014), with ModelFinder considering only the most likely 20% of partition schemes. Substitution models with I + G extensions to accommodate among-site rate heterogeneity were permitted, as version 1.4.3 onward of IQ-Tree implements an optimisation heuristic that effectively compensates for the non-identifiability of these models (Nguyen *et al.* 2018). Bayesian inference was performed in ExaBayes (ver. 1.5.1, see https://github.com/aberer/exabayes; Aberer *et al.* 2014) on the CIPRES Science Gateway under the partitioning scheme produced by ModelFinder in IQ-Tree (as described above) with GTR + G imposed across all partitions, all parameters unlinked, with the single Markov Chain Monte Carlo (MCMC) running until the average standard deviation of split frequencies (ASDSF) of topologies $< 0.05$, for 100 000 generations. Convergence of the MCMC with respect to continuous parameters was visually assessed in Tracer (ver. 1.7, see https://github.com/beast-dev/tracer/; Rambaut *et al.* 2018).

## Nomenclature

Nomenclature for sculpturation follows Harris (1979); setation, Wilson (1955) and Boudinot *et al.* (2020). Notation of palp and tibial spur formulae follows Bolton (2003). Cephalic nomenclature follows Richter *et al.* (2021) and Boudinot *et al.* (2021). Mesosomal nomenclature follows Liu *et al.* (2019); metasomal, Lieberman *et al.* (2022). Male genital nomenclature follows Boudinot (2018).

## Measurements

Sorting and initial examination of the material was done using an Echo-Lab SM203H stereomicroscope (DEVCO, Milan, Italy). Morphometric data for four specimens of *Y. laventa* are included in Table 2. Detailed morphological study of these specimens was performed with a Leica MZ75 compound

**Table 2.** Measurements and indices for the type series of *Yavnella laventa*.

| | CASENT0842746 | CASENT0842745 | CASENT0842747 | CASENT0842748 |
|---|---|---|---|---|
| Measurements (mm) | | | | |
| HW | 0.353 | N/A | 0.358 | 0.332 |
| HL | 0.491 | 0.512 | 0.497 | 0.490 |
| SL | 0.564 | 0.588 | 0.585 | 0.554 |
| MaL | 0.264 | 0.256 | 0.275 | 0.265 |
| WL | 0.844 | 0.820 | 0.848 | 0.736 |
| PrW | 0.199 | 0.228 | 0.214 | 0.211 |
| MW | 0.159 | 0.163 | 0.165 | 0.143 |
| PTL | 0.232 | 0.230 | 0.238 | 0.222 |
| PTH | 0.097 | 0.096 | 0.100 | 0.089 |
| PTW | 0.071 | 0.067 | 0.069 | 0.071 |
| PPL | 0.133 | 0.139 | 0.133 | 0.122 |
| PPW | 0.086 | 0.085 | 0.083 | 0.072 |
| PPH | 0.119 | 0.118 | 0.121 | 0.119 |
| Indices | | | | |
| CI | 71.894 | N/A | 72.032 | 68 |
| SI | 159.773 | N/A | 163.408 | 167 |
| MI | 53.768 | 50.000 | 55.332 | 80 |
| PI | 30.603 | 29.130 | 28.992 | 32 |
| PPI | 64.662 | 61.151 | 62.406 | 59 |
| PPHI | 72.269 | 72.034 | 68.595 | 98 |

microscope (Leica Microsystems, Oak Grove, IL, USA) at magnifications of up to 50×. Photographs were obtained as image stacks using a Leica DMC2900 camera attached to a Leica MZ16A stereomicroscope or using the Visionary Digital Imaging System (Visionary Digital, Richmond, VA, USA), with *z*-stepping in the Leica Application Suite (LAS) software (ver. 4.13.0, see https://www.leica-microsystems.com/products/microscope-software/p/leica-las-x-ls/) and montaged with Helicon Focus Pro (ver. 7.7.4, Helicon Software Ltd, Kharkiv, Ukraine). Scanning electron microscopy was performed with a Hitachi TM4000 (Hitachi Global, Tokyo, Japan). Measurement and index definitions are provided below.

HW, maximum width of cranium in full-face view.

HL, head length, maximum length of head in full-face view from anterior margin of head to cranial vertex.

SL, scape length, maximum length of scape in medial view, excluding bulbus.

MaL, mandible length, maximum length of mandible from view orthogonal to lateral mandibular margin, measured from ventral mandibular articulation to mandibular apex.

WL, Weber's length, maximum diagonal length of mesosoma in profile view, measured from most anterior extent of pronotum excluding cervical shield to most posterior extent of propodeal lobes, when present.

PrW, pronotal width, maximum width of pronotum, measured in dorsal view.

MW, mesonotal width, maximum width of mesonotum in dorsal view, measured immediately anterior to mesocoxal foramen.

PTL, petiolar length, maximum length of petiole in dorsal view, not including presclerites.

PTH, petiolar height, maximum height of petiole in profile view, including sternal process and dorsal node, if distinct.

PTW, petiolar width, maximum width of petiole in dorsal view.

PPL, postpetiolar length, maximum length of postpetiole in dorsal view, not including presclerites.

PPW, postpetiolar width, maximum width of postpetiole in dorsal view.

PPH, postpetiolar height, maximum height of postpetiole in profile view, including sternal process and dorsal node, if distinct.

### Indices

CI = (HW ÷ HL) × 100
SI = (SL ÷ HW) × 100
MI = (MaL ÷ HW) × 100
PI = (PTW ÷ PTL) × 100
PPI = (PPW ÷ PPL) × 100
PPHI = (PPH ÷ PPL) × 100

## Phylogeny

Maximum-likelihood phylogenomic inference from a 313 498-bp alignment consisting of 473 UCEs, partitioned within-locus, corroborates the phylogeny of Leptanillinae as recovered by Griebenow (2020). All nodes along the backbone of the tree are recovered with high support under ML, with sub-maximal UFBoot/SH-aLRT values being restricted to the sister-group relationships of two terminals within *Yavnella*. Phylogenomic inference under a Bayesian framework, partitioned using a scheme derived according to an information–theoretic criterion (BIC) using ModelFinder in IQ-Tree (ver. 2.1.2), recovers all internal nodes of the phylogeny with maximal Bayesian posterior probability (BPP), with nearly all estimated parameters having an effective sample size (ESS) of >200 (the exceptions with ESS = 190–191). *Yavnella laventa* is likewise robustly recovered within *Yavnella* with maximal support under ML and Bayesian frameworks (UFBoot, SH-aLRT = 100; BPP = 1) and sister to *Yavnella argamani* (UFBoot, SH-aLRT = 100; BPP = 1) (Fig. 2).

## Class **INSECTA** Linnaeus, 1758

## Order **HYMENOPTERA** Linnaeus, 1758

## Family **FORMICIDAE** Latreille, 1809

## Subfamily **LEPTANILLINAE** Emery, 1910

## Tribe **LEPTANILLINI** Emery, 1910

### Diagnosis (worker-based)

Palp formula 2,1 or 1,1. Mandible without differentiated basal and masticatory margins. Medial mandibular margin without regularly spaced serration (Fig. 3*c*, *d*). Peg-like chaetae absent from mandible and labrum. Clypeus without median demarcation from frons by posterior carina, anteroposteriorly compressed anterior to antennal toruli; antennal torulus adjacent to, or abutting, anterior margin of cranium (Fig. 3*c*, *d*); antennal socket fully exposed. Compound eye absent. Frontal carina absent. Antenna 12-merous. Promesonotal articulation highly flexible. Mesotibia with 0–2 apical spurs. Propodeal lobe absent; propodeal spiracle situated low on propodeum. Abdominal segments II–III with tergosternal fusion. Spiracle of abdominal segment III very large and placed far forward. Abdominal segment III posteriorly constricted, forming postpetiole (Fig. 4). Spiracles of abdominal segments IV–VII concealed by posterior margins of preceding tergites. Abdominal segment IV without tergosternal fusion; stridulitrum absent from abdominal presclerite IV. Abdominal tergite VII large, with simple posterior margin. Sting present. Pretarsal claw without apical tooth on inner margin.

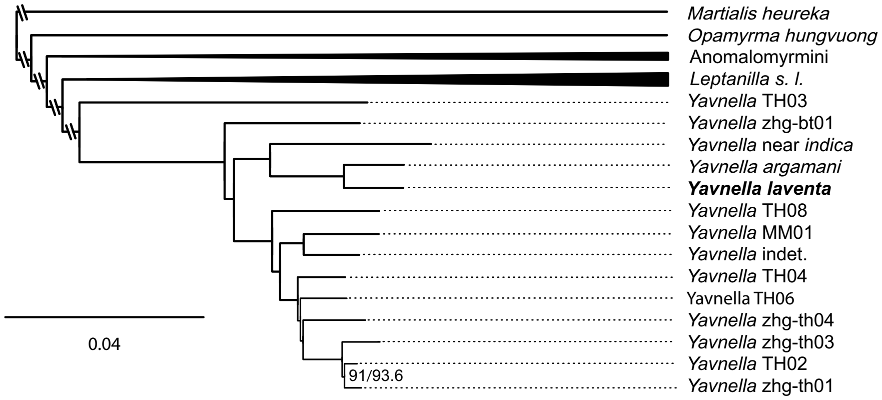

**Fig. 2.** Maximum-likelihood phylogeny of the Leptanillinae, inferred from an alignment of 473 ultra-conserved elements (UCEs) partitioned within-locus (Kalyaanamoorthy *et al.* 2017; Tagliacollo and Lanfear 2018) and rooted *a posteriori* on *Martialis heureka* as an outgroup. The Anomalomyrmini (9 terminals) and *Leptanilla s. l.* (26 terminals) are collapsed. Node support values are UFBoot/SH-aLRT and are only noted when <100. The phylogeny of the Leptanillinae inferred from the same data using a Bayesian approach was identical to the ML phylogeny shown here and is provided on Zenodo (doi:10.5281/zenodo.5595290). Branch length is expressed in number of expected substitutions per site.

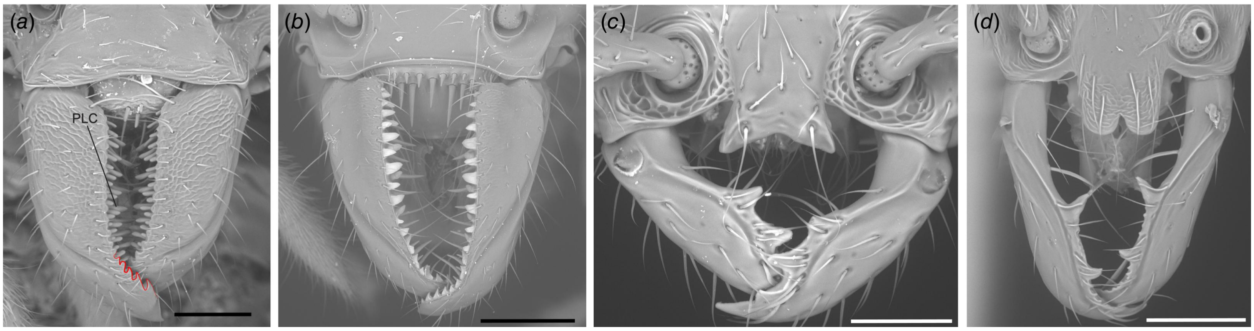

**Fig. 3.** Full-face view of mandibular armature across the Leptanillinae. (*a*) *Protanilla beijingensis* (CASENT0842639). Regular serration at mandibular apex outlined in red. (*b*) *Anomalomyrma* indet. (CASENT0178553). (*c*) *Leptanilla thai* (CASENT0842784). (*d*) *Yavnella laventa* (CASENT0842745). PLC, peg-like chaetae. Scale bars: *a*, *b*, 0.2 mm; *c*, 0.04 mm; *d*, 0.1 mm.

## Genus ***Yavnella*** Kugler, 1987

*Yavnella* Kugler, 1987 [published in a 1986 volume in Kugler 1986], p. 52. *Type species*: *Yavnella argamani*, original designation.

### Diagnosis (worker-based)

Three mandibular teeth present (Fig. 5*a*). Palp formula 2,1 (Fig. 5*c*). Mesotibia with 2 apical spurs. Petiole much longer than wide in dorsal view (PI ≤ 31) (Fig. 4), without distinct anterior peduncle. Abdominal segment IV constricted anteriorly in dorsal view; total length of abdominal segment IV greater than that of abdominal segments V–VII combined.

### Diagnosis (male-based)

Palp formula 1,1. Ocelli present and set on a distinct tubercle (Griebenow 2020, fig. 5A), rarely absent (Griebenow 2020, fig. 6A); if present, anteromedian ocellus orthogonally dorsal to compound eye in profile view (Griebenow 2020, fig. 12Bi). Procoxa without distal transverse carina (cf. Petersen 1968, p. 583, fig. 8). Protrochanter not elongated relative to meso- and metatrochanter. Profemur without sinuate medial carina or ventral hook. Medioventral carina (Griebenow 2021, fig. 1) and comb (Griebenow 2021, fig. 3) absent from protibia. Notauli absent. Pronotum and mesoscutum not anteroposteriorly elongated. Pterostigma absent (Griebenow 2020, fig. 4B). Recurved posteroventral process absent from mesoscutellum (Griebenow 2021, fig. 16A). Lower metapleuron indistinct. Propodeal declivity concave in profile view (Griebenow 2021, fig. 19B); propodeum without dorsolateral carina. Petiole reduced, without distinct dorsal node. Abdominal tergite VIII broader than long in posterodorsal view. Volsellae present, not dorsoventrally compressed and lamellate; fully articulated medially; parossiculus and lateropenite not distinguishable. Phallotreme apical, not surrounded with dense vestiture of setae.

## ***Yavnella laventa*** Griebenow, Moradmand & Isaia, sp. nov.

(Fig. 4–11)

ZooBank: urn:lsid:zoobank.org:act:1BCBAA0B-753E-4DD4-8CFA-43CC25BCE68E

## Material examined

*Holotype.* Iran, Fārs: **1.3 km E Khoorab** [in *Milieu Souterrain Superficiel*], 60 cm [below surface], 28.59843°N, 52.32863°E [±10 m], alt. 620 m, MSS2, 14.II.2019-26.VI.2020, M. Isaia & M. Moradmand leg. (ZMHB CASENT0842746), ♀.

*Paratypes.* Iran, Fārs: **1.3 km E Khoorab** [in *Milieu Souterrain Superficiel*], 60 cm [below surface], 28.59843°N, 52.32863°E [±10 m], alt. 620 m, MSS2, 14.II.2019-26.VI.2020, M. Isaia & M. Moradmand leg., 1 ♀ (ZMUI CASENT0842745); **ibid.**, 3 ♀ (ZMUI CASENT0842747, ZMUI CASENT0842795, ZMUI CASENT0842796); **ibid.**, 1 ♀ (JAZM CASENT0842797); **1.3 km E Khoorab** [in *Milieu Souterrain Superficiel*], 100 cm [below surface], 28.59841°N, 52.32856°E [±10 m], alt. 618 m, MSS4, 14.II.2019-26.VI.2020, M. Isaia & M. Moradmand leg., 1 ♀ (ZMHB CASENT0842748).

*Other material examined.* Iran, Fārs: **1.3 km E Khoorab** [in *Milieu Souterrain Superficiel*], 60 cm [below surface], 28.59843°N, 52.32863°E [±10 m], alt. 620 m, MSS2, 14.II.2019-26.VI.2020, M. Isaia & M. Moradmand leg., 1 ♀ (head and hind leg) (ZMHB CASENT0842789); **ibid.**, 1 ♀ (mesothorax and metapectal-propodeal complex with hind leg) (ZMHB CASENT0842790).

## Diagnosis (worker-based)

As for genus (see above).

## Diagnosis (male-based)

Male unknown.

**Fig. 4.** Propodeum and abdominal segments II–IV of *Yavnella laventa* (CASENT0842746), dorsal view. Scale bar: 0.1 mm.

## Etymology

Named after *La Venta Esplorazioni Geografiche*, the organisation that facilitated the 2019 faunal survey of south-western Iranian salt caves and their vicinity, during which

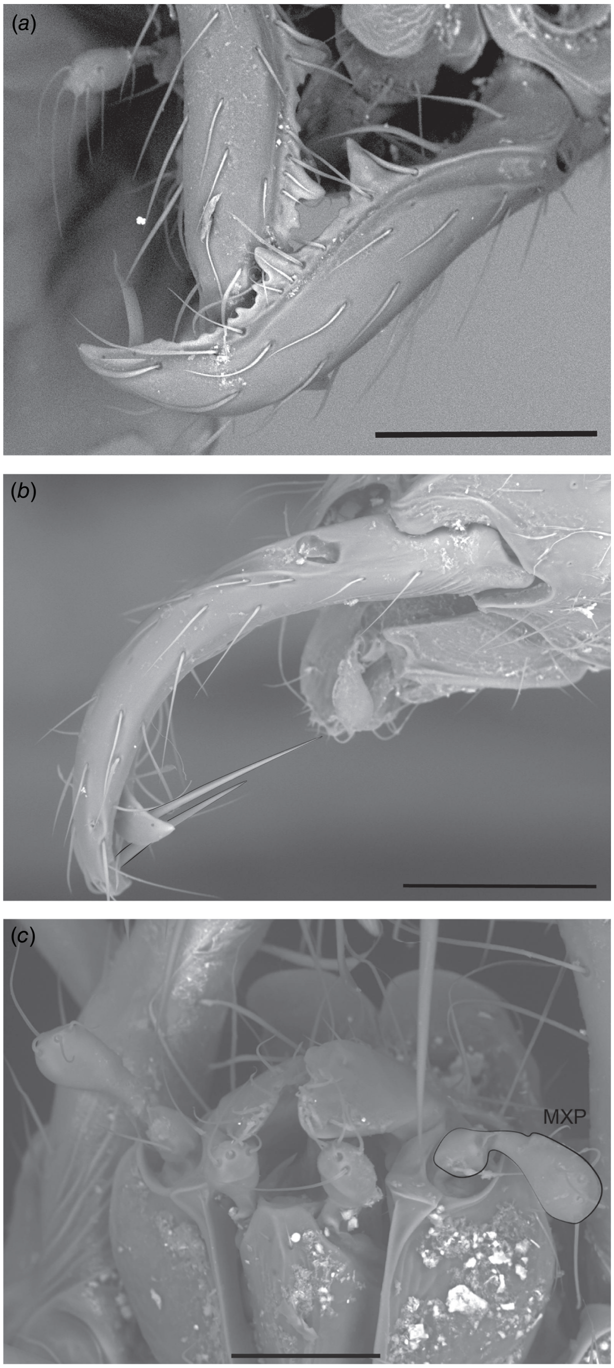

**Fig. 5.** Mouthparts of *Yavnella laventa*. (*a*) Mandibles, dorsal oblique view (CASENT0842789). (*b*) Mandibles, profile view (CASENT0842748). Putative 'trigger hairs' outlined in black. (*c*) Mouthparts of *Yavnella laventa*, ventral view (CASENT0842789). Maxillary palp (MXP) outlined in black. Scale bars: *a*, *b*, 0.1 mm; *c*, 0.05 mm.

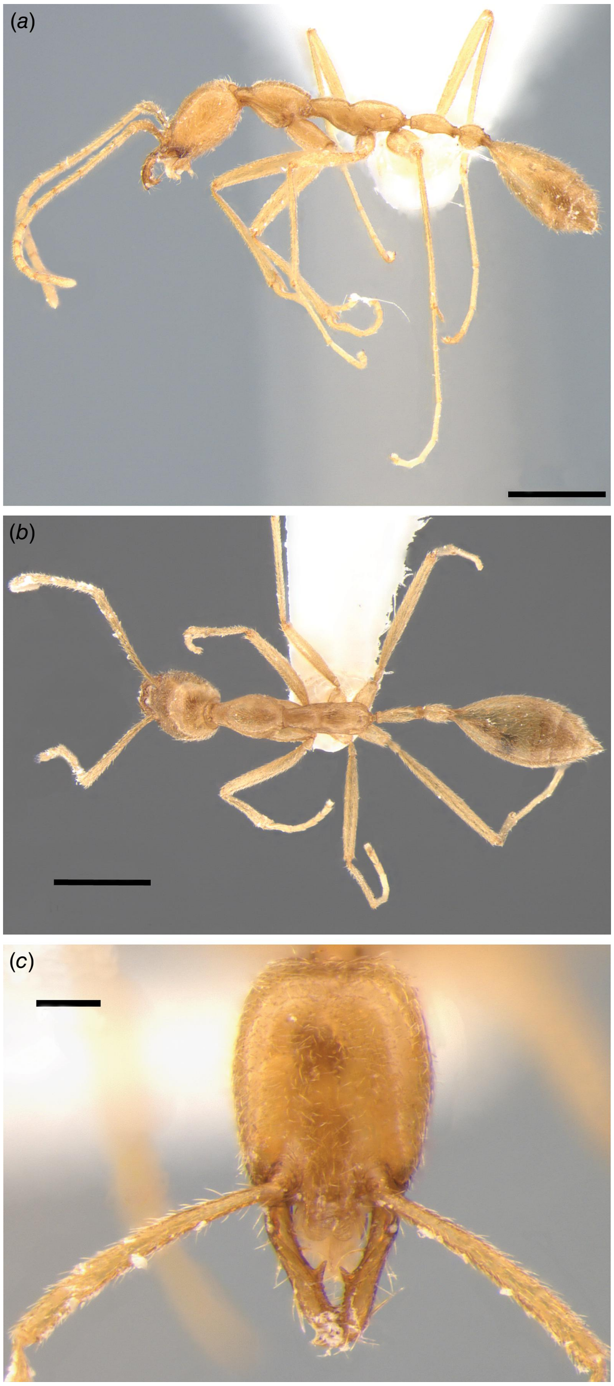

**Fig. 6.** *Yavnella laventa*, holotype (CASENT0842746). (*a*) Profile view. (*b*) Dorsal view. (*c*) Full-face view. Scale bars: *a*, *b*, 0.5 mm; *c*, 0.1 mm.

the type series of this species was collected. The specific epithet is a noun in apposition and is therefore invariant.

## Description

### Head

Cranium longer than wide in full-face view (CI = 68–72). In full-face view, vertex of cranium emarginate;

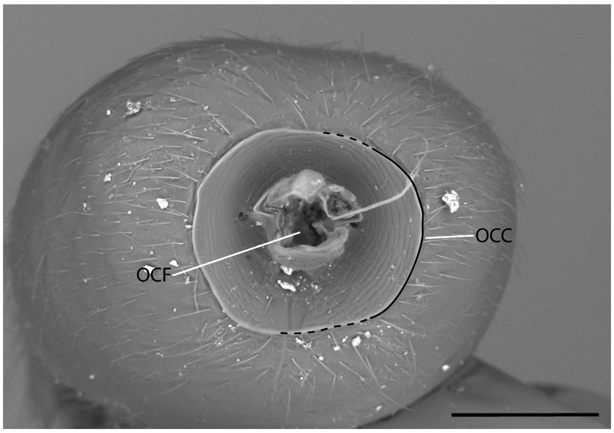

**Fig. 7.** Cranium of *Yavnella laventa* (CASENT0842789), posterior view. OCC, occipital carina; OCF, occipital foramen. Scale bar: 0.1 mm.

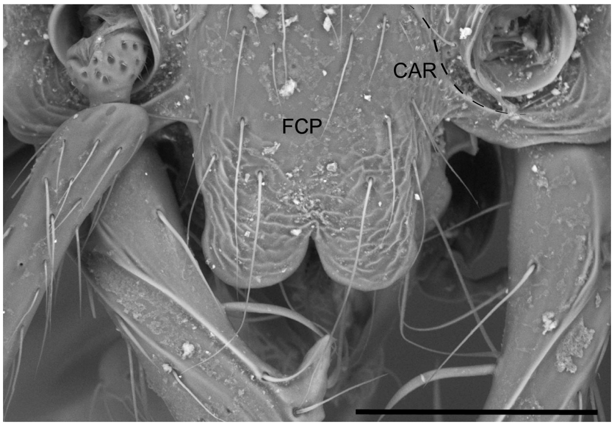

**Fig. 8.** Frontoclypeal process of *Yavnella laventa* (CASENT0842789), full-face view. CAR, lateral carina; FCP, frontoclypeal process. Scale bar: 0.1 mm.

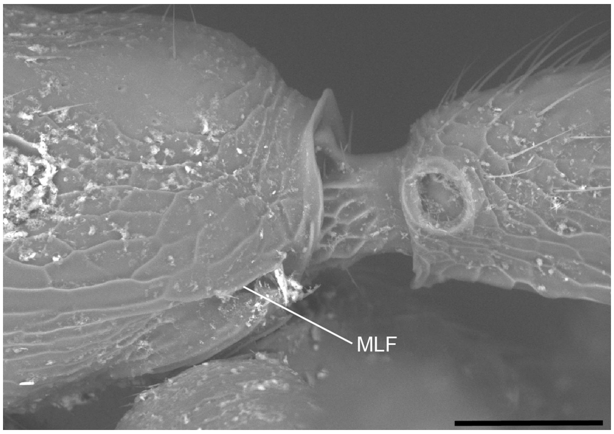

**Fig. 9.** Propodeum and anterior petiole of *Yavnella laventa* (CASENT0842745), profile view. MLF, metapleural longitudinal flange. Scale bar: 0.05 mm.

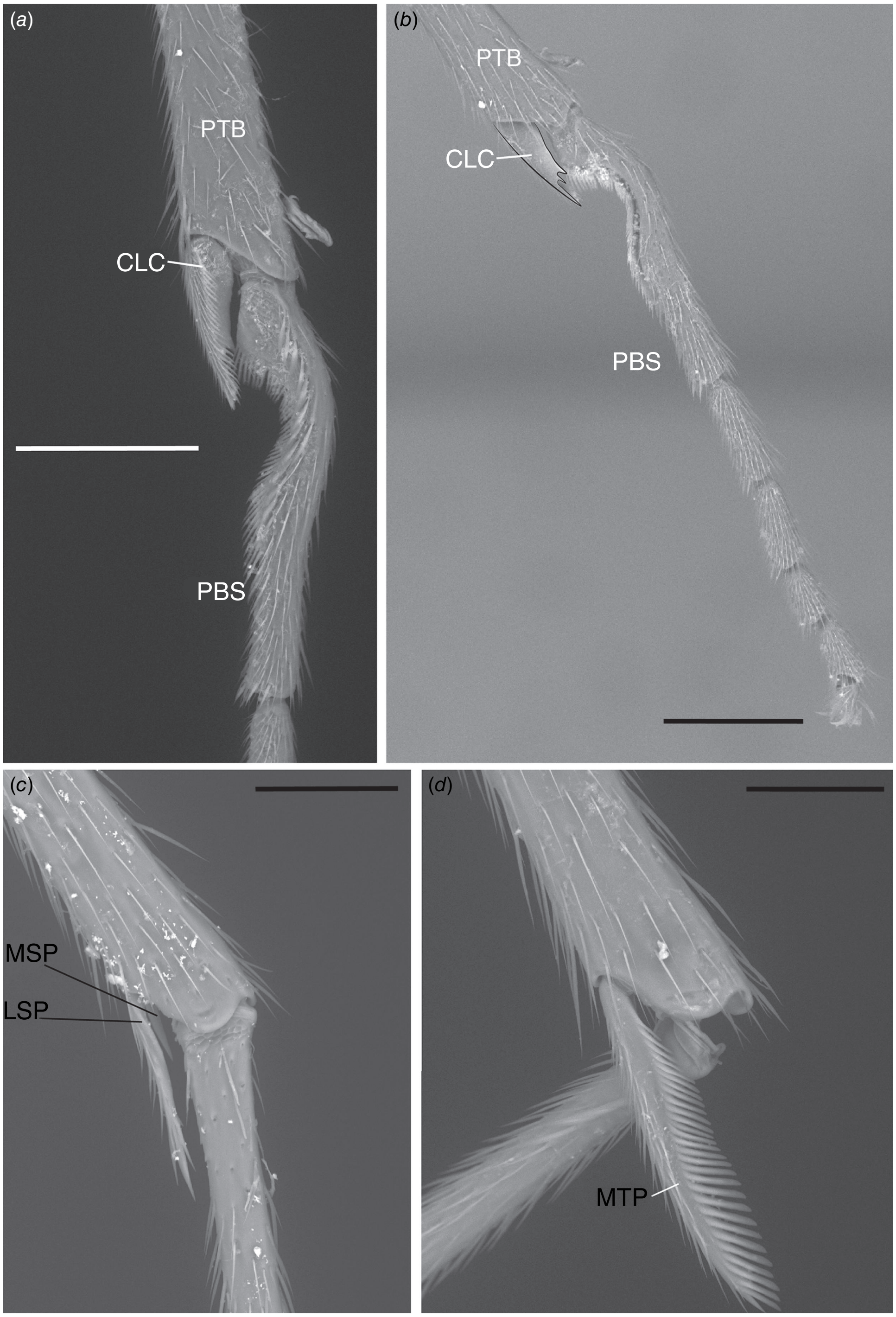

**Fig. 10.** Tibial spurs of *Yavnella laventa*. (*a*) Antennal strigil, anterior view (CASENT0842745). (*b*) Protarsus, posterior view; calcar outlined (CASENT0842745). (*c*) Mesotibia and mesobasitarsus, posterior view (CASENT0842746). (*d*) Metatibial spur (CASENT0842789), posterior view. CLC, calcar; PTB, protibia; PBS, probasitarsus; MSP, anterior mesotibial spur; LSP, posterior mesotibial spur; MTP, metatibial spur. Scale bars: *a*, 0.1 mm; *b*, 0.2 mm; *c*, 0.05 mm; *d*, 0.1 mm.

occiput anteroposteriorly narrow, occipital carina completely encircling occipital foramen (Fig. 7). Lateral margins of cranium slightly convex. Frontal carina absent. Antennal insertion exposed. Frontoclypeal process present, delimited from cranium by lateral carinae (Fig. 8), without posteromedian delimitation from cranium, projecting well anterior of labrum in full-face view; frontoclypeal process laminate, broad in outline, with apex emarginate, and anterolateral corners

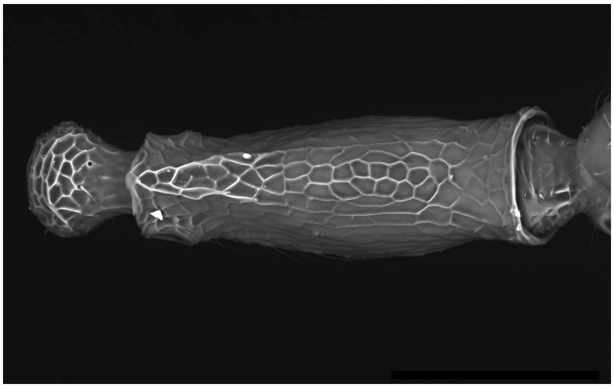

**Fig. 11.** Ventral view of abdominal sternite II of *Yavnella laventa* (CASENT0842745). Scale bar: 0.1 mm.

lobate (Fig. 8). Clypeus anteroposteriorly compressed anterior to antennal toruli; epistomal sulcus absent.

Anterior tentorial pit not visible. Antennal torulus circular. Hypostomal carina present. Postgenal ridge extending from hypostoma to occipital carina. Mandible projecting anteriorly at rest (Fig. 3*d*). Mandalus small and bean-shaped in outline. Lateral mandibular groove extending along 1/3 of mandible surface, with a smaller groove laterad the longitudinal line, beginning at the basal tooth; both grooves merging proximad subapical tooth. Medial mandibular margin not divided into basal and masticatory portions. Three teeth present on mandible, apical tooth acute; basal tooth larger than subapical tooth, tip recurved; margin distal to subapical tooth irregularly serrate (Fig. 5*a*). Large, tapering basal and subapical setae present on mandible (Fig. 5*b*). Peg-like chaetae absent from mandible. Labrum concealed by frontoclypeal process in full-face view; peg-like chaetae absent from labrum. Palp formula 2,1 (Fig. 5*c*). Ventral premental face elliptical. Antennae 12-merous. Scape elongated, extending well beyond cranial vertex at rest (SI = 160–163); margins subparallel, slightly expanded towards apex. Pedicel longer than broad; constriction separating pedicel from flagellum not pronounced. Flagellum filiform; all flagellomeres longer than broad, with antennomere 3 longer than length of any of the distal antennomeres (Fig. 6*a, b*); apex of antennomere 12 slightly tapered.

### Mesosoma

In dorsal view, pronotal outline anteroposteriorly oblate, maximum width (PrW = 0.199–0.228) greater than that of mesonotum, or of the propodeum (Fig. 6*b*). Pronotal dorsum convex, elevated above dorsal mesonotal vertex. Promesonotal suture present, highly flexible. Mesonotum constricted anteriorly in dorsal view, with maximum width < PrW (Fig. 6*b*); indistinct from mesopleural region. Mesothorax dorsoventrally constricted and anteroposteriorly elongated posterad the promesonotal suture in profile view (Fig. 6*a*). Meso-metapleural suture absent; in profile view, fusion of mesonotum with propodeum marked by excavation. Propodeum not constricted anteriorly in dorsal view, with outline subrectangular. Metapleural gland bulla large, anterior margin extending slightly anterior to anterior margin of propodeal spiracle. Metapleural gland orifice longitudinally elongated, curving posteriorly towards dorsum, overhung by longitudinal flange (Fig. 9).

Propodeal declivity convex in profile view. Coxae robust, pro- and mesocoxae well separated; distal leg articles elongated (Fig. 10*b*). Metacoxal dorsum unarmed. Tibial spur formula 2b,1p. Calcar large, anterior margin densely pectinated (Fig. 10*a*), posterior surface bare, velum large; apex of posterior margin with two subapical spines (Fig. 10*b*); posterior stout seta absent from protibia. Anterior mesotibial spur reduced, barbulate with slight splintering; posterior mesotibial spur with pronounced barbulation. Metatibial spur pectinate (Fig. 10*d*). Meso- and metabasitarsus less than one half the length of meso- and metatibia, respectively. Anterior surface of probasitarsus with single row of acute scale-like cuticular processes (Fig. 10*a*); posterior surface bare of such processes. Tarsomeres with traction chaetae small and restricted to distal margins. Pretarsal claws unarmed, length less than that of tarsomere 5. Arolium present.

### Metasoma

Anterior margin of petiole linear in dorsal view. Abdominal spiracle II very large, situated well forward on petiole. Petiole much longer than wide (PI = 29–32) (Fig. 4), without distinct dorsal node or ventral process; sessile; tergosternal fusion complete, with anterior ½ of abdominal sternite II delimited by longitudinal carinae, converging anteriorly in ventral view (Fig. 11); lateral margins subparallel in dorsal view. Dorsal and ventral surfaces of petiole shallowly convex in profile view. Abdominal spiracle III very large, situated well forward on postpetiole. Abdominal segment III posteriorly constricted, forming postpetiole; somewhat longer than wide (PPI = 59–65); tergosternal fusion complete, with longitudinal sutures not converging anteriorly in ventral view; lateral margins convex in dorsal view (Fig. 4). Prora distinct. Abdominal segment IV longer than length of posterior abdominal segments combined, constricted into 'neck' immediately posterior to abdominal segment III. Abdominal segments IV–VIII without tergosternal fusion. Abdominal sternite VII entire and unarmed. Sting well developed.

### Integument

Somal surface smooth to scabrous; mostly scabriculous. Anterior margins of pronotum, meso- and metapleuron, and abdominal sternite II areolate (Fig. 11) to rugose. Occiput substrigulose (Fig. 7). Appendages mostly unsculptured. Colouration orangish-yellow, extremities paler. Cuticle covered with short setae, subdecumbent to appressed; sparse on cranium, mesosoma, and abdominal sternite II. Setae longest on abdominal segments III and V–VII.

## Distribution

*Yavnella laventa* is known only from the type locality, inhabiting the MSS within a debris flow on the bank of an ephemeral stream adjacent to a salt diapir (Fig. 12). The Khoorab Salt Dome is one of ~130 salt diapirs occurring in southern Iran (Talbot and Alavi 1996). It is therefore possible that *Y. laventa* occurs across this area, at least in microhabitats resembling those present at the type locality.

## Habitat

Mean annual precipitation around the type locality is ~400 mm (Zarei 2010), meaning that moisture is a limiting abiotic factor. Microclimatic conditions in the MSS at the type locality were not directly measured becuase of data logger malfunction. Indeed, RH in the MSS is rarely measured for this reason (Mammola *et al.* 2016). Contrary to cave habitats, in which RH is generally constant, studies of this parameter in the MSS show seasonal variation, with a drop in spring through summer (Barranco *et al.* 2013). Using a data logger and measuring RH in the nearby salt cave (the 'Last Cave'), we found that RH varied seasonally from 50 to 80%, contrasting with the humidity and climatic constancy commonly associated with subterranean habitats (Cigna 2002; Badino 2010). We hypothesise that the hygroscopic property of salt causes a strong drop in humidity inside Last Cave, which may account for the absence of *Y. laventa*.

## Key to genera of the Leptanillinae based on the worker caste

1. Abdominal segment III not constricted posteriorly (Fig. 13*a*); occiput visible in full-face view (Yamada *et al.* 2020, fig. 1*a*).......................................................*Opamyrma* Yamane, Bui & Eguchi, 2008
– Abdominal segment III constricted posteriorly, forming postpetiole (Fig. 13*b*, *c*); occiput not visible in full-face view........................2
2. Posterior face of dorsal petiolar node not distinct (Fig. 13*c*); abdominal segments II-III with tergotergal and sternosternal fusion partial to complete..............*Anomalomyrma* Taylor in Bolton (1990)
– Posterior face of dorsal petiolar node distinct (Fig. 13*b*); abdominal segments II-III without tergotergal or sternosternal fusion..........3
3. Mandible with peg-like chaetae on medial face (Fig. 3*a*); mandible with regularly spaced dorsomedial serration; mandible lacking subapical teeth (Fig. 3*a*, *b*)......*Protanilla* Taylor in Bolton (1990)
– Mandible without peg-like chaetae on medial face; serration present *or* absent from dorsomedial margin (Fig. 3*c*, *d*), *if* present *then* irregularly spaced; mandible with ≥1 subapical tooth...............4
4. Frontoclypeal process present *or* absent (Fig. 14*a*), *if* present apex entire (Fig. 14*b*) *or* emarginate, *if* emarginate *then* apicolateral

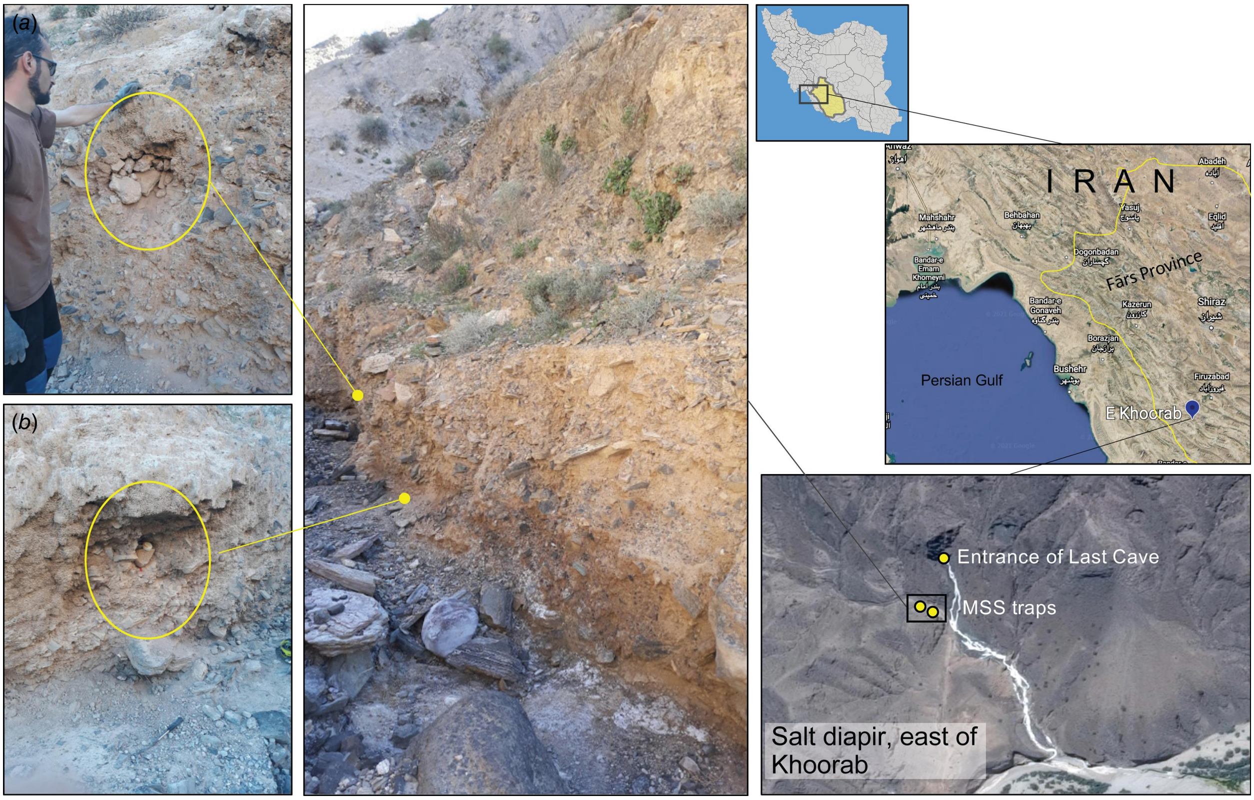

**Fig. 12.** Map of the type locality within Iran, and the spatial relationship of the MSS traps in which *Yavnella laventa* was collected relative to each other and to Last Cave. Yellow marks indicate approximate positions of MSS traps, which were located below the surface of the ground. (*a*) Location of MSS2. (*b*) Location of MSS4.

margins angular (Fig. 14*c*); SI < 100; PI > 31..............................
..................................................................*Leptanilla* Emery, 1870

– Frontoclypeal process present, apex emarginate, apicolateral margins lobate (Fig. 14*d*); SI ≥ 100; PI ≤ 31......*Yavnella* Kugler, 1987

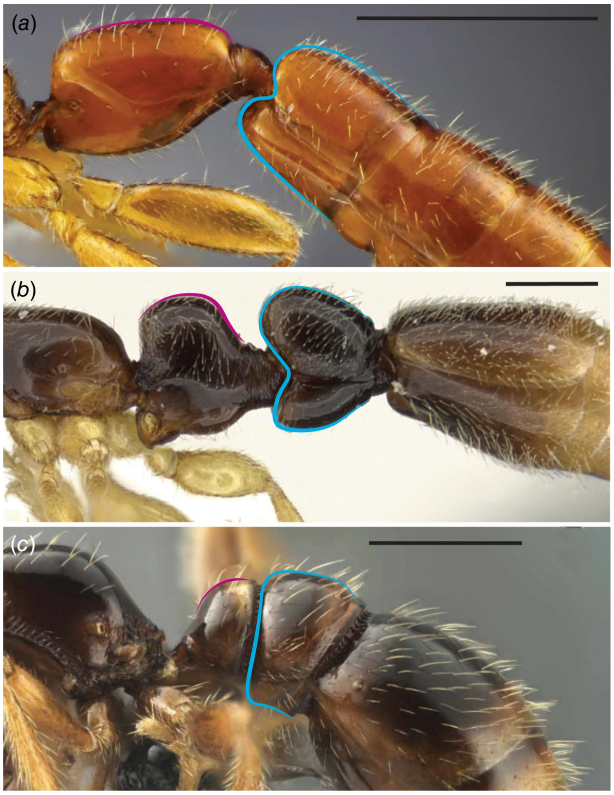

**Fig. 13.** Profile view of abdominal segments II–III across the Leptanillinae. Profile of abdominal tergite II outlined in magenta; profile of abdominal segment III outlined in blue. (*a*) *Opamyrma hungvuong* (AKY05vii17-06) (Yamada *et al.* 2020, fig. 1C). (*b*) *Protanilla bicolor* (CASENT0235341), Estella Ortega (AntWeb, ver. 8.68.7, California Academy of Sciences, see https://www.antweb.org). (*c*) *Anomalomyrma helenae* (CASENT0220220) (Borowiec *et al.* 2011, fig. 6). Scale bars: *a*, 0.5 mm; *c*, 0.2 mm; *c*, 0.5 mm.

# Discussion

## Morphology

The habitus of *Y. laventa* is exceptional among worker Leptanillinae in the elongation of the appendages, including the scape (Table 3), flagellomeres, and tarsomeres (Fig. 6*c*, 15*b*). The anterior constriction of abdominal segment IV is also unique among the Leptanillinae, exceeding the constriction observed in *Leptanilla tanakai* Baroni Urbani, 1977 (Baroni Urbani 1977, fig. 33). *Protanilla* spp. have long scapes (SI > 100) by comparison to *Leptanilla* (Richter *et al.* 2021), but these are less elongated than in *Y. laventa* (Table 3). Elongation of the scapes in *Protanilla* was hypothesised to be a secondary reversal from the ancestral condition in the Leptanillini (Richter *et al.* 2021). This implies that the elongation of the scape in *Y. laventa* is also a secondary reversal.

The elongation of appendicular articles in *Y. laventa* is unparalleled in the 'leptanillomorph clade', i.e. *Martialis* + Leptanillinae (Borowiec *et al.* 2019; Richter *et al.* 2021), as is the elongation of the petiole (PI = 29–32) (Tables 2, 3). Leptanillomorph workers generally have robust, short limbs, with a submoniliform antennal funiculus; this tendency is most pronounced in the Leptanillini. Along with positioning of the antennal toruli anterior to their ancestral position for the Formicidae, shortening of extremities is associated with motion in confined subterranean conditions (Eisenbeis and Wichard 1987; Richter *et al.* 2021). By contrast, the extremities of *Y. laventa* are attenuated and fragile, with the antennal funiculus filiform. This convincingly restricts this species to subterranean voids, as predicted for *M. heureka* (Rabeling *et al.* 2008, fig. 2). The sparseness of traction chaetae on the ventral tarsal surface (Fig. 10*b*, 15*b*) also implies limited digging capability in *Y. laventa* compared to examined *Leptanilla* spp. (Fig. 15).

The emarginate frontoclypeal process of *Y. laventa* resembles that observed in many *Leptanilla* spp., mostly

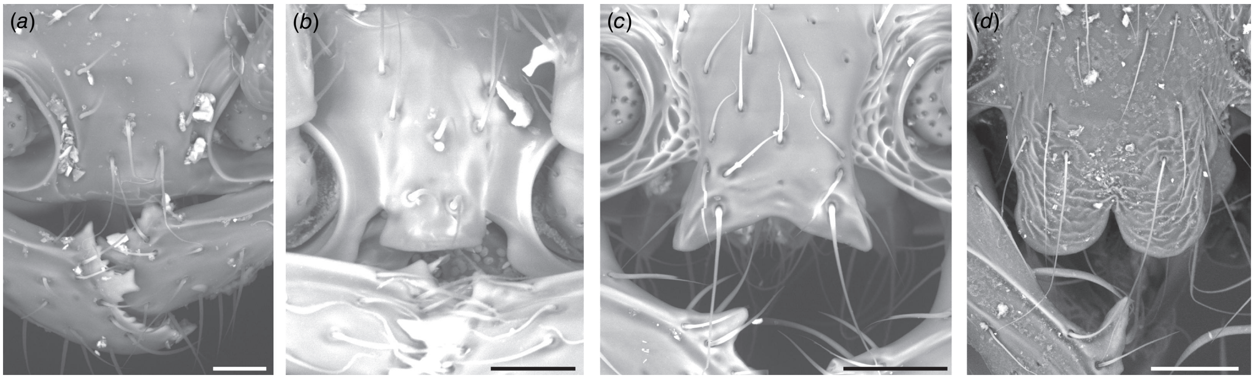

**Fig. 14.** Full-face view of the frontoclypeal margin across the tribe Leptanillini. (*a*) *Leptanilla* KE01 (CASENT0842721). (*b*) *Leptanilla boltoni* (CASENT0260440). (*c*) *Leptanilla thai* (CASENT0842784). (*d*) *Yavnella laventa* (CASENT0842789). Scale bars: *a*, *b*, 0.02 mm; *c*, 0.035 mm; *d*, 0.05  mm.

**Table 3.** Comparison of scape index (SI) and petiole index (PI) in *Yavnella laventa* to that observed in a selection of other leptanillomorph species.

| Species | SI | PI | Reference |
|---|---|---|---|
| *Yavnella laventa* (*n* = 4) | 160–163[A] | 29–31 | This study |
| *Martialis heureka* (*n* = 1) | 72 | 70 | Rabeling *et al.* (2008) |
| *Protanilla flamma* (*n* = 2) | 86–90 | 110–112 | Baidya and Bagchi (2020) |
| *Leptanilla plutonia* (*n* = 20) | 64–72 | 66–77 | Pérez-González *et al.* (2020) |
| *Leptanilla hypodracos* (*n* = 2) | 69 | 60[B] | Wong and Guénard (2016) |
| *Leptanilla macauensis* (*n* = 4) | 49–56 | 84–88 | Leong *et al.* (2018) |

[A] *n* = 3.
[B] *n* = 1.

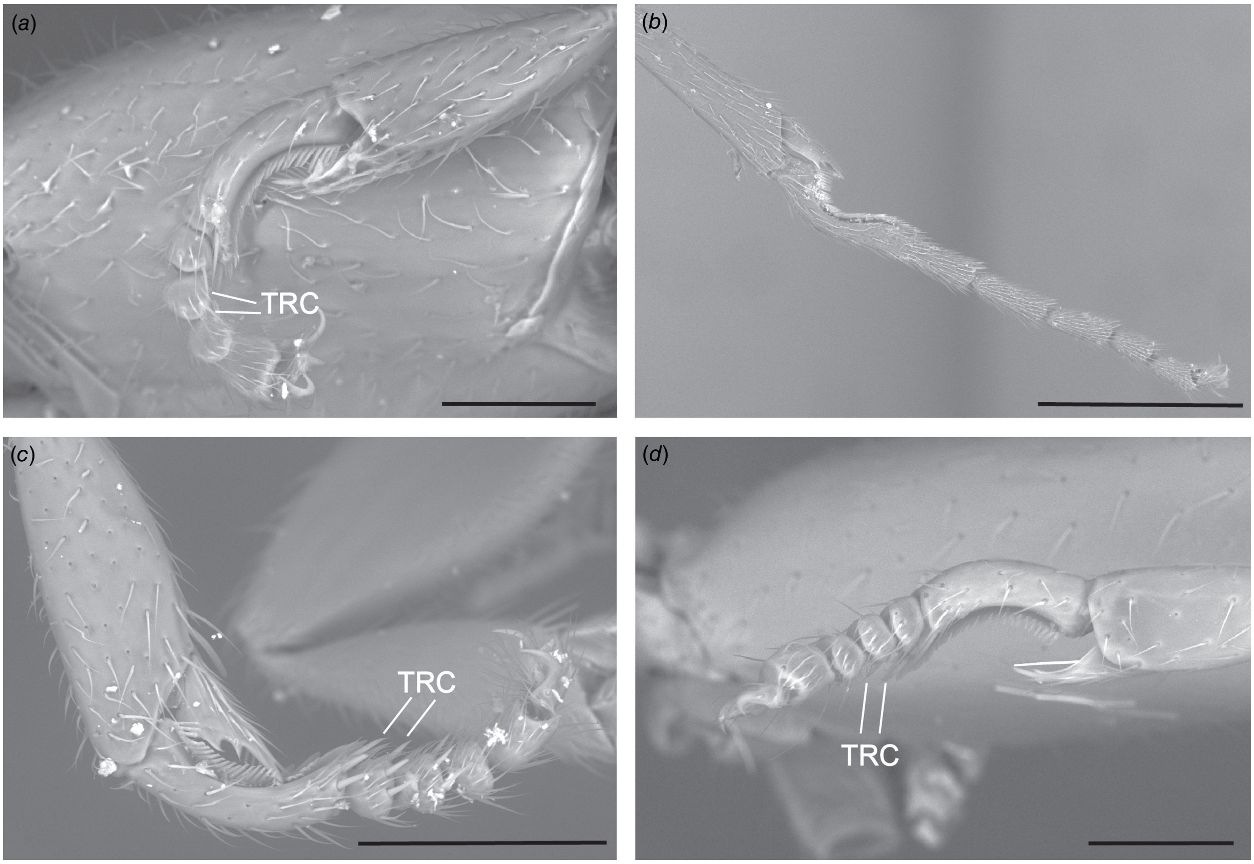

**Fig. 15.** Protarsi of selected *Leptanilla* spp. and *Yavnella laventa*, lateral view. (*a*) *Leptanilla boltoni* (CASENT0842753). (*b*) *Yavnella laventa* (CASENT0842745). (*c*) *Leptanilla thai* (CASENT0842752). (*d*) *Leptanilla theryi* (CASENT0842751). TRC, traction chaetae. Scale bars: *a*, 0.05 mm; *b*, 0.2 mm; *c*, 0.1 mm; 0.05 mm.

distributed in the Indo-Malayan ecoregion. Although regarded as clypeal in origin by previous authors (e.g. Leong *et al.* 2018), the homology of the frontoclypeal process is unclear, since it is difficult to delimit the clypeus in the absence of the epistomal sulcus.

The mandibular surface of *Y. laventa* bears sparse, tapering suberect setae of mostly uniform length and diameter. Two pairs of more robust, longer suberect setae are present on the medial mandibular surface, with the distal pair positionally homologous with the putative 'trigger hairs' present in *Protanilla lini* and *Protanilla rafflesi* Taylor in Bolton (1990) (Richter *et al.* 2021). This is the first purported example of trigger hairs in the Leptanillini. The definition of trigger hairs has always been functional rather than anatomical, relying upon confirmation of 'trap-jaw' behaviour, or assertion by analogy to other ants for which behavioural observations exist (e.g. Creighton 1930; Barden and Grimaldi 2012; Richter *et al.* 2021). Observations of living *Y. laventa*, or three-dimensional modelling of mandibular movement in this species based upon micro-CT data, would test the hypothesised function of these mandibular setae (cf. Richter *et al.* 2021). Consultation of the primary literature (e.g. Man *et al.* 2017, fig. 5; Aswaj *et al.* 2020, fig. 2C; Baidya and Bagchi 2020, fig. 1C), photographs on AntWeb (ver. 8.68.7, California Academy of Sciences, see https://www.antweb.org), and available specimens showed that the subapical mandibular seta is present and robust in all described species of Anomalomyrmini for which this information is available. The presence of a robust subapical mandibular seta was also confirmed in all available undescribed specimens of that tribe (Table 4). There were few available worker specimens belonging to the Leptanillini in which mandibular setation could be assessed. A subapical mandibular seta is present in those that were examined and in *O. hungvuong* (Yamada *et al.* 2020, fig. 2E) (Table 4) but is less produced than in the Anomalomyrmini or *Y. laventa*, leaving its function as a trigger hair doubtful.

In *Y. laventa* the mandibles are elongated such that, when closed, these rest in a position subparallel to the anteroposterior axis of the cranium (Fig. 3*d*, 5*b*, 6*c*), resembling the Anomalomyrmini. This is not a condition previously observed in the Leptanillini. Save for the posture of the mandibles at rest, *Y. laventa* has little morphological commonality with the Anomalomyrmini to the exclusion of other Leptanillini. Anomalomyrmine workers are uniformly distinguished from the Leptanillini, including *Yavnella*, by the presence of four maxillary palpomeres; the presence of regular serration on the medial mandibular margin, and absence of large teeth from that margin; the presence of at least one peg-like chaeta on the labrum; and the median demarcation of the clypeus from the frons by a carina.

## Ecology

*Yavnella laventa* was collected ≥60 cm. below the surface, setting the workers of this species apart from other Leptanillinae for which soil depth of origin is recorded: these workers approach the depths of *Y. laventa* only in *Leptanilla taiwanensis* Ogata, Terayama & Masuko, 1995 and *Protanilla beijingensis* Man, Ran, Chen & Zhu, 2017 have been collected with unbaited pitfall traps at depths of up to 55 cm (Man *et al.* 2017).

The biotope of *Y. laventa* appears to be the MSS, rather than soil as is the case in other leptanilline ants, which is consistent with the strikingly gracile phenotype of this species. The elongated, delicate limbs preclude the endogean (i.e. soil dwelling) biology otherwise observed in this subfamily, instead indicating hypogean habits. This elongation of extremities is consistent with troglomorphism. Worker Leptanillinae lack compound eyes, and so that condition in *Y. laventa* does not constitute troglomorphism *per se*, although it corroborates our supposition that this species is exclusively subterranean, as are all other leptanilline ants. Rather, the argument for troglomorphism in *Y. laventa* rests upon overall elongation of the extremities in conjunction with subterranean biology. This is analogous to troglomorphic Japygidae and Campodeidae (Hexapoda: Diplura), which likewise belong to an ancestrally eyeless, endogean clade, and differ from endogean relatives by larger size and elongation or multiplication of appendicular articles (Sendra *et al.* 2021). A similar pattern is also recovered in subterranean spiders (Araneae), e.g. *Troglohyphantes* spp. (Linyphiidae), in which leg length appears to correlate with habitat (pore) size (Mammola and Isaia 2016).

We here follow the definition of Bichuette *et al.* (2015) for troglomorphism, regarding it as constituting phenotypic traits selectively favoured by subterranean biology and apomorphic relative to non-subterranean relatives of the putatively troglomorphic lineage. By this definition, troglomorphism does not necessarily coincide with habitation in subterranean voids that are considered caves by dint of being ‘commensurable to the human scale’ (Mammola *et al.* 2016, p. 3). Therefore, that *Y. laventa* was collected in the MSS does not exclude its being troglomorphic. Indeed, this condition is unsurprising, since troglomorphic organisms are frequently encountered in the MSS (Christiansen 2005; Juberthie and Decu 2006; see Mammola *et al.* 2016 for further evidence from the literature).

Few ants are known to reside permanently in caves (Pape 2016) or exhibit troglomorphism (Christiansen 2005). Whereas *Nylanderia pearsei* Wheeler, 1938 (Formicinae: Lasiini) from the Yucatán Peninsula and an undescribed *Leptogenys* sp. (Ponerinae: Ponerini) from central Texas are subterranean so far as is known (Wheeler 1938; Reddell 1977; Cokendolpher *et al.* 2009), neither is unambiguously troglomorphic in phenotype. Compelling arguments for troglomorphism among described ants have heretofore only been made for *Leptogenys khammouanensis* and *Aphaenogaster gamagumayaa*. When compared to their respective closest relatives, both display a gracile habitus, pale colouration and reduced compound eyes (Roncin and Deharveng 2003; Naka and Maruyama 2018). Additionally, *L. khammouanensis* was collected in two large calcareous caves in Laos, ranging from 500 m to several kilometres from the cave entrance (Roncin and Deharveng 2003), whereas *A. gamagumayaa* was collected ~20 m within a calcareous cave on Okinawa, apparently nesting in the floor of an aphotic guano hall (Naka and Maruyama 2018, pp. 138–139).

## Generic classification

Since *Y. laventa* is the sole species of *Yavnella* for which the worker has been identified, the range of morphological variation in the worker caste of *Yavnella* is unknown, as is the prevalence of troglomorphism in *Yavnella*. If all that is required for the evolution of troglomorphism in the

**Table 4.** Presence or absence of a subapical mandibular seta in all described species belonging to the tribe Anomalomyrmini, and in 8 specimens belonging to undescribed morphospecies of this tribe.

| Specimen identifier | Species identification | Subapical mandibular seta | Reference |
|---|---|---|---|
| CASENT0178553 | *Anomalomyrma* indet. | Present | This study |
| CASENT0217032 | *Anomalomyrma boltoni* | Present | Borowiec *et al.* (2011, fig. 2) |
| CASENT0220221 | *Anomalomyrma helenae* | Present | Borowiec *et al.* (2011, p. 6) |
| CASENT0101976 | *Anomalomyrma taylori* | Present | Borowiec *et al.* (2011, fig. 12) |
| CASENT0842753 | *Leptanilla boltoni* | Present | This study |
| CASENT0010809 | *Leptanilla havilandi* | Present | This study |
| CASENT0842784 | *Leptanilla thai* | Present | This study |
| AKY05vii17-06 | *Opamyrma hungvuong* | Present | Yamada *et al.* (2020, fig. 2E) |
| CASENT0106383 | *Protanilla* indet. | Present | This study |
| CASENT0898001 | *Protanilla* indet. | Present | AntWeb, see https://www.antweb.org/specimen/CASENT0898001 |
| CASENT0842639 | *Protanilla beijingensis* | Present | This study |
| CASENT0235341 | *Protanilla bicolor* | Present | AntWeb (2022) |
| – | *Protanilla concolor* | ? | Not examined |
| CESM-198516 | *Protanilla flamma* | Present | Baidya and Bagchi (2020, fig. 1C) |
| – | *Protanilla furcomandibula* | Present | Xu (2012, p. 481) |
| – | *Protanilla gengma* | Present | Aswaj *et al.* (2020, fig. 2C) |
| CASENT0842850 | *Protanilla izanagi* | Present | This study |
| CASENT0824693 | *Protanilla jongi* | Present | This study |
| CASENT0709417 | *Protanilla lini* | Present | Richter *et al.* (2021, fig. 6D, 7A) |
| CASENT0746018 | *Protanilla* MY01 | Present | AntWeb, see https://www.antweb.org/specimen/CASENT0746018 |
| CASENT0842640 | *Protanilla* psw-my01 | Present | This study |
| CASENT0842972 | *Protanilla rafflesi* | Present | Richter *et al.* (2021) |
| CASENT0911228 | *Protanilla schoedli* | Present | Baroni Urbani and de Andrade (2006, p. 45) |
| – | *Protanilla tibeta* | Present | Xu (2012, p. 488) |
| CASENT0179564 | *Protanilla* VN01 | Present | This study |
| CASENT0179565 | *Protanilla* VN03 | Present | This study |
| CASENT0842699 | *Protanilla wallacei*[A] | Present | This study |
| CASENT0221924 | *Protanilla wardi* | Present | This study |
| CASENT0842745 | *Yavnella laventa* | Present | This study |

Also included are *Opamyrma hungvuong* and the only three species of the Leptanillini for which mandibular setation could be examined.
[A] *Nomen nudum*.

Leptanillinae is the presence of the MSS, troglomorphism could be prevalent across the worker caste in *Yavnella*, since the geographical extent of the MSS is unknown (Juberthie and Decu 2006; Mammola *et al.* 2016).

It must be cautioned that without troglomorphic elongation of the soma and extremities, and putative trigger hairs, workers of *Y. laventa* cannot be discriminated from those of *Leptanilla*. Disregarding these apomorphies, the phenotype of *Y. laventa* shows close affinity to *Leptanilla escheri* (Kutter, 1948) and *Leptanilla judaica* Kugler, 1987. The 2,1 palp formula of *Y. laventa* (Fig. 5c) resembles that in *Leptanilla havilandi* Forel, 1901, *L. escheri*, *L. judaica*, and *Leptanilla ujjalai* Saroj *et al.*, 2022 (this study; Kugler 1986; Saroj *et al.* 2022), whereas the anteromedian frontoclypeal process of *Y. laventa* resembles that observed in these and other *Leptanilla* spp. (Kugler 1986; Wong and Guénard

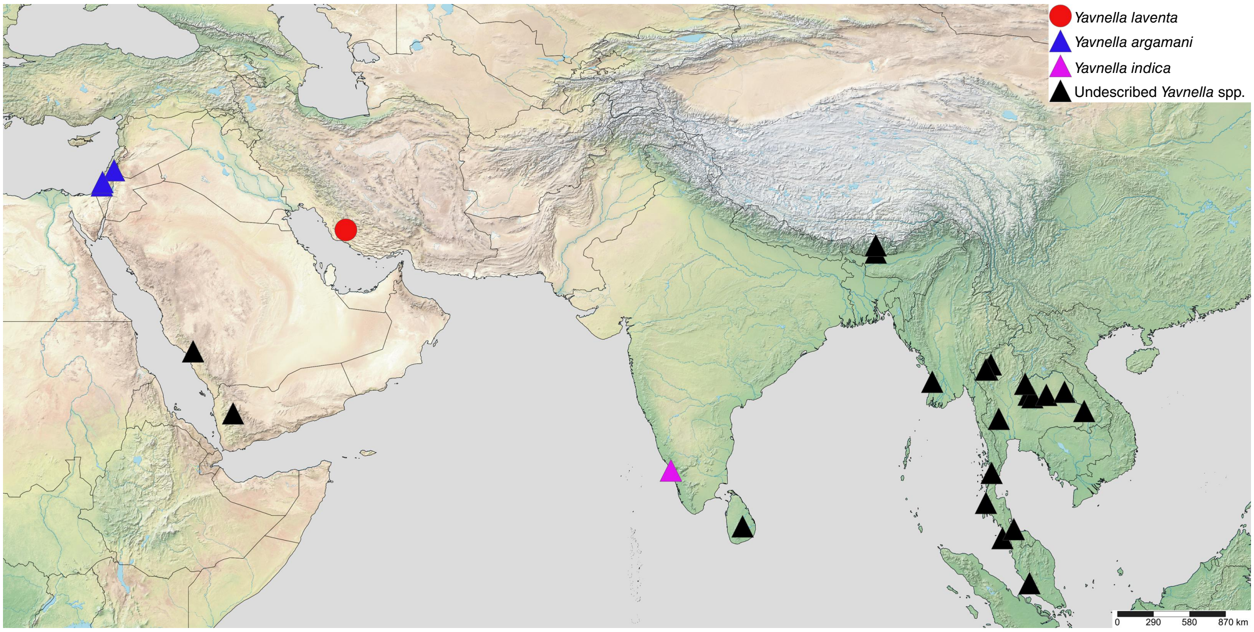

**Fig. 16.** Distribution of known specimens attributed to *Yavnella*, according to Collingwood and Agosti (1996) and AntWeb (see https://www.antweb.org), with generic attribution of undescribed morphospecies following Griebenow (2021). Generated using SimpleMappr (https://www.simplemappr.net).

2016, fig. 1A, B; Leong *et al.* 2018, fig. 14B, C, 15A; Saroj *et al.* 2022, fig. 3B).

It is possible that *L. escheri* and *L. judaica* are non-troglomorphic representatives of *Yavnella*. In the absence of molecular data for *L. escheri*, *L. judaica* or their close relatives *Leptanilla lamellata* Bharti & Kumar, 2012 and *L. ujjalai*, we refrain from transferring any *Leptanilla* spp. to *Yavnella.* The hypothesis that these *Leptanilla* spp. represent *Yavnella* has biogeographical plausibility, because these species are known from the Indian subcontinent and Israel, with Iran intervening between these regions (Fig. 16). Under this hypothesis, it is plausible that *Yavnella indica* Kugler, 1987 and *Y. argamani* respectively represent the males of *L. escheri* and *L. judaica*, a prediction that could be tested with molecular data, as in this study and others (e.g. Ward and Brady 2009; Griebenow 2020).

Identification of *L. escheri* or any of its relatives as representatives of *Yavnella* would erase the distinction between that genus and *Leptanilla* in the worker caste. The subapical mandibular setae have not been comprehensively surveyed across the known diversity of the Leptanillini and therefore are not of monothetic use. *Yavnella* and *Leptanilla s. l.* are uniformly discriminated based upon male morphology (Griebenow 2021) and robustly recovered as reciprocally monophyletic by ML and Bayesian phylogenomic inference (Griebenow 2020, 2021; this study). Resolving the taxonomic status of the major subclades of the Leptanillini, including *Yavnella*, will require sequencing of further worker material across this tribe, including the as-yet-unknown worker caste of *Scyphodon*, *Noonilla,* and the undescribed Bornean morphospecies-group (Griebenow 2020, 2021).

## Supplementary material

Supplementary material is available online.

## References

Abbassi HR, Aleni MR, Feiznia S, Darvish M, Ahmadian M, Shahbazi A (2015) Effects of geological formation on desertification in the Mond watershed. *Iranian Journal of Range & Desert Research* **22**(3), 583–593. [In Farsi]

Aberer AJ, Kobert K, Stamatakis A (2014) ExaBayes: massively parallel Bayesian tree inference for the whole-genome era. *Molecular Biology and Evolution* **31**(10), 2553–2556. doi:10.1093/molbev/msu236

Aswaj P, Anoop K, Priyadarsanan DR (2020) First record of the rarely collected ant *Protanilla gengma* Xu, 2012 (Hymenoptera, Formicidae, Leptanillinae) from the Indian subcontinent. *Check List* **16**(6), 1621–1625. doi:10.15560/16.6.1621

Badino G (2010) Underground meteorology – "what's the weather underground?" *Acta Carsologica* **39**, 427–448. doi:10.3986/ac.v39i3.74

Baidya P, Bagchi S (2020) A new species of *Protanilla* Taylor 1990 (Hymenoptera: Formicidae: Leptanillinae) from India. *Halteres* **11**, 19–24. doi:10.5281/zenodo.3941686

Bankevich A, Nurk S, Antipov D, Gurevich AA, Dvorkin M, Kulikov AS, Lesin VM, Nikolenko SI, Pham S, Prjibelski AD, Pyshkin AV, Sirotkin AV, Vyahhi N, Tesler G, Alekseyev MA, Pevzner PA (2012) SPAdes: a new genome assembly algorithm and its applications to single-cell sequencing. *Journal of Computational Biology* **19**(5), 455–477. doi:10.1089/cmb.2012.0021

Barden P, Grimaldi D (2012) Rediscovery of the bizarre Cretaceous ant *Haidomyrmex* Dlussky (Hymenoptera: Formicidae), with two new species. *American Museum Novitates* **3755**, 1–16. doi:10.1206/3755.2

Baroni Urbani C (1977) Materiali per una revisione della sottofamiglia Leptanillinae Emery (Hymenoptera: Formicidae). *Entomologica Basiliensia* **2**, 427–488. [In Italian]

Baroni Urbani C, de Andrade ML (2006) A new *Protanilla* Taylor, 1990 (Hymenoptera: Formicidae: Leptanillinae) from Sri Lanka. *Myrmecologische Nachrichten* **8**, 45–47.

Barranco P, Gilgado JD, Ortuño VM (2013) A new mute species of the genus *Nemobius* Serville (Orthoptera, Gryllidae, Nemobiinae) discovered in colluvial, stony debris in the Iberian Peninsula: a biological, phenological and biometric study. *Zootaxa* **3691**(2), 201–219. doi:10.11646/zootaxa.3691.2.1

Bichuette ME, Rantin B, Hingst-Zaher E, Trajano E (2015) Geometric morphometrics throws light on evolution of the subterranean catfish *Rhamdiopsis krugi* (Teleostei: Siluriformes: Heptapteridae) in eastern Brazil. *Biological Journal of the Linnean Society* **114**, 136–151. doi:10.1111/bij.12405

Billen J, Bauweleers E, Hashim R, Ito F (2013) Survey of the exocrine system in *Protanilla wallacei* (Hymenoptera, Formicidae). *Arthropod Structure & Development* **42**(3), 173–183. doi:10.1016/j.asd.2013.01.001

Bolton B (1990) The higher classification of the ant subfamily Leptanillinae (Hymenoptera: Formicidae). *Systematic Entomology* **15**, 267–282. doi:10.1111/j.1365-3113.1990.tb00063.x

Bolton B (2003) Synopsis and classification of Formicidae. *Memoirs of the American Entomological Institute* **71**, 1–370.

Borowiec ML (2016) AMAS: a fast tool for alignment manipulation and computing of summary statistics. *PeerJ* **4**, e1660. doi:10.7717/peerj.1660

Borowiec ML, Schulz A, Alpert GD, Baňař P (2011) Discovery of the worker caste and descriptions of two new species of *Anomalomyrma* (Hymenoptera: Formicidae: Leptanillinae) with unique abdominal morphology. *Zootaxa* **2810**, 1–14. doi:10.11646/zootaxa.2810.1.1

Borowiec ML, Rabeling C, Brady SG, Fisher BL, Schultz TR, Ward PS (2019) Compositional heterogeneity and outgroup choice influence the internal phylogeny of the ants. *Molecular Phylogenetics and Evolution* **134**, 111–121. doi:10.1016/j.ympev.2019.01.024

Boudinot BE (2018) A general theory of genital homologies for the Hexapoda (Pancrustacea) derived from skeletomuscular correspondences, with emphasis on the Endopterygota. *Arthropod Structure & Development* **47**(6), 563–613. doi:10.1016/j.asd.2018.11.001

Boudinot BE, Perrichot V, Chaul JCM (2020) †*Camelosphecia* gen. nov., lost ant-wasp intermediates from the mid-Cretaceous (Hymenoptera, Formicoidea). *ZooKeys* **1005**, 21–55. doi:10.3897/zookeys.1005.57629

Boudinot BE, Moosdorf OTD, Beutel RG, Richter A (2021) Anatomy and evolution of the head of *Dorylus helvolus* (Formicidae: Dorylinae): patterns of sex- and caste-limited traits in the sausagefly and the driver ant. *Journal of Morphology* **282**, 1616–1658. doi:10.1002/jmor.21410

Branstetter MG, Longino JT, Ward PS, Faircloth BC (2017) Enriching the ant tree of life: enhanced UCE bait set for genome-scale phylogenetics of ants and other Hymenoptera. *Methods in Ecology & Evolution* **8**(6), 768–776. doi:10.1111/2041-210X.12742

Castresana J (2000) Selection of conserved blocks from multiple alignments for their use in phylogenetic analysis. *Molecular Biology and Evolution* **17**(4), 540–552. doi:10.1093/oxfordjournals.molbev.a026334

Chernomor O, von Haeseler A, Minh BQ (2016) Terrace aware data structure for phylogenomic inference from supermatrices. *Systematic Biology* **65**(6), 997–1008. doi:10.1093/sysbio/syw037

Christiansen KA (2005) Morphological adaptations. In 'Encyclopedia of Caves'. (Eds D Culver, WB White) pp. 517–527. (Elsevier: Amsterdam, Netherlands)

Cigna AA (2002) Modern trend [*sic*] in cave monitoring. *Acta Carsologica* **31**, 35–54. [In English with Slovenian abstract]

Cokendolpher JC, Reddell JR, Taylor SJ, Krejca JK, Suarez AV, Pekins CE (2009) Further ants (Hymenoptera: Formicidae) from caves of Texas. In 'Studies on the Cave & Endogean Fauna of North America. Vol. 7'. (Eds JC Cokendolpher, JR Reddell) pp. 151–168. (University of Texas at Austin: Austin, TX, USA)

Collingwood CA, Agosti D (1996) Formicidae (Insecta: Hymenoptera) of Saudi Arabia (part 2). *Fauna of Saudi Arabia* **15**, 300–385.

Creighton WS (1930) A review of the genus *Myrmoteras* (Hymenoptera: Formicidae). *Journal of the New York Entomological Society* **38**, 177–192.

Cruaud A, Nidelet S, Arnal P, Weber A, Fusu L, Gumovsky A, Huber J, Polaszek A, Rasplus J-Y (2019) Optimized DNA extraction and library preparation for minute arthropods: application to target enrichment in chalcid wasps used for biocontrol. *Molecular Ecology Resources* **19**(3), 702–710. doi:10.1111/1755-0998.13006

Culver DC, Pipan T (2014) 'Shallow Subterranean Habitats: Ecology, Evolution, & Conservation.' (Oxford University Press: New York, NY, USA)

Eisenbeis G, Wichard W (1987) 'Atlas on the Biology of Soil Arthropods.' (Springer: Berlin, Germany)

Emery C (1910) Hymenoptera. Fam. Formicidae. Subfam. Dorylinae. *Genera Insectorum* **102**, 1–34.

Faircloth BC (2016) PHYLUCE is a software package for the analysis of conserved genomic loci. *Bioinformatics* **32**(5), 786–788. doi:10.1093/bioinformatics/btv646

Griebenow ZH (2020) Delimitation of tribes in the subfamily Leptanillinae (Hymenoptera: Formicidae), with a description of the male of *Protanilla lini* Terayama, 2009. *Myrmecological News* **30**, 229–250. doi:10.25849/myrmecol.news_030:229

Griebenow ZH (2021) Synonymisation of the male-based ant genus *Phaulomyrma* (Hymenoptera : Formicidae) with *Leptanilla* based upon Bayesian total-evidence phylogenetic inference. *Invertebrate Systematics* **35**, 603–636. doi:10.1071/IS20059

Guindon S, Dufayard JF, Lefort V, Anisimova M, Hordijk W, Gascuel O (2010) New algorithms and methods to estimate maximum-likelihood phylogenies: assessing the performance of PhyML 3.0. *Systematic Biology* **59**(3), 307–321. doi:10.1093/sysbio/syq010

Harris RA (1979) A glossary of surface sculpturing. *Occasional Papers in Entomology* **28**, 1–31.

Hoang DT, Chernomor O, von Haeseler A, Minh BQ, Vinh LS (2018) UFBoot2: improving the ultrafast bootstrap approximation. *Molecular Biology and Evolution* **35**(2), 518–522. doi:10.1093/molbev/msx281

Hölldobler B, Wilson EO (1990) 'The Ants.' (Harvard University Press: Cambridge, MA, USA)

Hsu P-W, Hsu F-C, Hsiao Y, Lin CC (2017) Taxonomic notes on the genus *Protanilla* (Hymenoptera: Formicidae: Leptanillinae) from Taiwan. *Zootaxa* **4268**(1), 117–130. doi:10.11646/zootaxa.4268.1.7

Ito F, Yamane S (2020) Behavior of the queen of *Leptanilla clypeata* Yamane *et* Ito collected in the Bogor Botanical Gardens, West Java, Indonesia (Hymenoptera; Formicidae), with a note on colony composition and a description of the ergatoid queen. *Asian Myrmecology* **12**, e012004. doi:10.20362/AM.012004

Ito F, Hashim R, Mizuno R, Billen J (2022) Notes on the biology of *Protanilla* sp. (Hymenoptera, Formicidae) collected in Ulu Gombak, Peninsular Malaysia. *Insectes Sociaux* **69**, 13–18. doi:10.1007/s00040-021-00839-z

Juberthie C, Decu V (2006) Interstitial habitat (terrestrial). In 'Encyclopedia of Caves & Karst Science'. (Ed J Gunn) pp. 984–987. (Taylor and Francis Group: New York, NY, USA)

Kalyaanamoorthy S, Minh BQ, Wong TKF, von Haeseler A, Jermiin LS (2017) ModelFinder: fast model selection for accurate phylogenetic estimates. *Nature Methods* **14**(6), 587–589. doi:10.1038/nmeth.4285

Katoh K, Toh H (2010) Parallelization of the MAFFT multiple sequence alignment program. *Bioinformatics* **26**(15), 1899–1900. doi:10.1093/bioinformatics/btq224

Kugler J (1986) The Leptanillinae (Hymenoptera: Formicidae) of Israel and a description of a new species from India. *Israel Journal of Entomology* **20**, 45–47. [Published in 1987]

Lanfear R, Calcott B, Kainer D, Mayer C, Stamatakis A (2014) Selecting optimal partitioning schemes for phylogenomic datasets. *BMC Evolutionary Biology* **14**, 82. doi:10.1186/1471-2148-14-82

Leong C-M, Yamane S, Guénard B (2018) Lost in the city: discovery of the rare ant genus *Leptanilla* (Hymenoptera: Formicidae) in Macau with description of *Leptanilla macauensis* sp. nov. *Asian Myrmecology* **10**, e010001. doi:10.20362/am.010001

Lieberman ZE, Billen J, van de Kamp T, Boudinot BE (2022) The ant abdomen: the skeletomuscular and soft tissue anatomy of *Amblyopone australis* workers (Hymenoptera: Formicidae). *Journal of Morphology* **283**, 693–770. doi:10.1002/jmor.21471

Liu SP, Richter A, Stoessel A, Beutel RG (2019) The mesosomal anatomy of *Myrmecia nigrocincta* workers and evolutionary transformations in Formicidae (Hymenoptera). *Arthropod Systematics & Phylogeny* **77**(1), 1–19.

Mammola S, Isaia M (2016) The ecological niche of a specialized subterranean spider. *Invertebrate Biology* **135**(1), 20–30. doi:10.1111/ivb.12113

Mammola S, Giachino PM, Piano E, Jones A, Barberis M, Badino G, Isaia M (2016) Ecology and sampling techniques of an understudied subterranean habitat: the *Milieu Souterrain Superficiel* (MSS). *The Science of Nature* **103**, 88. doi:10.1007/s00114–016–1413–9

Man P, Ran H, Chen Z, Xu Z (2017) The northernmost record of Leptanillinae in China with description of *Protanilla beijingensis* sp. nov. (Hymenoptera: Formicidae). *Asian Myrmecology* **9**, e009008. doi:10.20362/am.009008

Masuko K (1990) Behavior and ecology of the enigmatic ant *Leptanilla japonica* Baroni Urbani (Hymenoptera: Formicidae: Leptanillinae). *Insectes Sociaux* **37**, 31–57.

Miller MA, Pfeiffer W, Schwartz T (2010) Creating the CIPRES Science Gateway for inference of large phylogenetic trees. In 'Proceedings of the Gateway Computing Environments Workshop (GCE)', 14 November 2010, New Orleans, LA, USA. INSPEC Accession Number 11705685. (IEEE) doi:10.1109/GCE.2010.5676129

Minh BQ, Schmidt HA, Chernomor O, Schrempf D, Woodhams MD, von Haeseler A, Lanfear R (2020) IQ-TREE 2: new models and efficient methods for phylogenetic inference in the genomic era. *Molecular Biology and Evolution* **37**(5), 1530–1534. doi:10.1093/molbev/msaa015

Naka T, Maruyama M (2018) *Aphaenogaster gamagumayaa* sp. nov.: the first troglobiotic ant from Japan (Hymenoptera: Formicidae: Myrmicinae). *Zootaxa* **4450**(1), 135–141. doi:10.11646/zootaxa.4450.1.10

Nguyen L-T, von Haeseler A, Minh BQ (2018) Complex models of sequence evolution require accurate estimators as exemplified with the invariable site plus gamma model. *Systematic Biology* **67**(3), 552–558. doi:10.1093/sysbio/syx092

Ogata K, Terayama M, Masuko K (1995) The ant genus *Leptanilla*: discovery of the worker-associated male of *L. japonica*, and a description of a new species from Taiwan (Hymenoptera: Formicidae: Leptanillinae). *Systematic Entomology* **20**(1), 27–34. doi:10.1111/j.1365-3113.1995.tb00081.x

Pape R (2016) The importance of ants in cave ecology, with new records and behavioral observations of ants in Arizona caves. *International Journal of Speleology* **45**(3), 185–205. doi:10.5038/1827-806X.45.3.1936

Pérez-González S, Gómez-Durán JM, Martínez-Ibáñez MD (2020) Highlighting the elusive: new findings and a redescription of the rare ant *Leptanilla plutonia* López, Martínez *et* Barandica, 1994, presenting morphological novelties for the genus. *Annales Zoologici* **70**(2), 289–304. doi:10.3161/00034541ANZ2020.70.2.009

Petersen B (1968) Some novelties in presumed males of Leptanillinae (Hym., Formicidae). *Entomologiske Meddelelser* **36**, 577–598. doi:10.5281/zenodo.25739

Rabeling C, Brown JM, Verhaagh M (2008) Newly discovered sister lineage sheds light on early ant evolution. *Proceedings of the National Academy of Sciences* **105**(39), 14913–14917. doi:10.1073/pnas.0806187105

Rambaut A, Drummond AJ, Xie D, Baele G, Suchard MA (2018) Posterior summarization in Bayesian phylogenetics using Tracer 1.7. *Systematic Biology* **67**(5), 901–904. doi:10.1093/sysbio/syy032

Reddell JR (1977) A preliminary survey of the caves of the Yucatan peninsula. In 'Studies of the Caves & Cave Fauna of the Yucatan Peninsula'. (Ed. JR Reddell) *Association for Mexican Cave Studies Bulletin*, Vol. 6, pp. 215–296. (Speleo Press: Austin, TX, USA)

Richter A, Garcia FH, Keller RA, Billen J, Katzke J, Boudinot BE, Economo EP, Beutel RG (2021) The head anatomy of *Protanilla lini* (Hymenoptera: Formicidae: Leptanillinae), with a hypothesis of their mandibular movement. *Myrmecological News* **31**, 81–114. doi:10.25849/myrmecol.news_031:085

Roncin E, Deharveng L (2003) *Leptogenys khammouanensis* sp. nov. (Hymenoptera: Formicidae). A possible troglobitic species of Laos, with a discussion on cave ants. *Zoological Science* **20**(7), 919–924. doi:10.2108/zsj.20.919

Saroj S, Mandi A, Dubey A (2022) A new species of the rare ant genus, *Leptanilla* Emery (Hymenoptera: Formicidae) from Eastern Himalaya, India. *Asian Myrmecology* **15**, e015005. doi:10.20362/am.015005

Sendra A, Komerički A, Lips J, Luan Y, Selfa J, Jiménez-Valverde A (2021) Asian cave-adapted diplurans, with the description of two new genera and four new species (Arthropoda, Hexapoda, Entognatha). *European Journal of Taxonomy* **731**, 1–46. doi:10.5852/ejt.2021.731.1199

Tagliacollo VA, Lanfear R (2018) Estimating improved partitioning schemes for ultraconserved elements. *Molecular Biology and Evolution* **35**(7), 1798–1811. doi:10.1093/molbev/msy069

Talbot CJ, Alavi M (1996) The past of a future syntaxis across the Zagros. *Geological Society, London, Special Publications* **100**, 89–109. doi:10.1144/GSL.SP.1996.100.01.08

Uéno SI (1980) The anophthalmic trechine beetles of the group of *Trechiama oshimai*. *Bulletin of the National Science Museum of Tokyo, Series A* **6**(4), 195–274.

Ward PS, Blaimer BB (2022) Taxonomy in the phylogenomic era: species boundaries and phylogenetic relationships among North American ants of the *Crematogaster scutellaris* group. *Zoological Journal of the Linnean Society* **194**(3), 893–937. doi:10.1093/zoolinnean/zlab047

Ward PS, Brady SG (2009) Rediscovery of the ant genus *Amyrmex* Kusnezov (Hymenoptera: Formicidae) and its transfer from Dolichoderinae to Leptanilloidinae. *Zootaxa* **2063**, 46–54. doi:10.11646/zootaxa.2063.1.2

Ward PS, Fisher BL (2016) Tales of dracula ants: the evolutionary history of the ant subfamily Amblyoponinae (Hymenoptera: Formicidae). *Systematic Entomology* **41**, 683–693. doi:10.1111/syen.12186

Wheeler WM (1938) Ants from the caves of Yucatan. In 'Fauna of the Caves of Yucatan'. (Ed. AS Pearse) pp. 251–255. (Carnegie Institution of Washington: Washington, DC, USA)

Wilson EO (1955) A monographic revision of the ant genus *Lasius*. *Bulletin of the Museum of Comparative Zoology* **113**, 1–201.

Wong MKL, Guénard B (2016) *Leptanilla hypodracos* sp. n., a new species of the cryptic ant genus *Leptanilla* (Hymenoptera, Formicidae) from Singapore, with new distribution data and an updated key to Oriental *Leptanilla* species. *ZooKeys* **551**, 129–144. doi:10.3897/zookeys.551.6686

Xu Z-H (2012) *Furcotanilla*, a new genus of the ant subfamily Leptanillinae from China with descriptions of two new species of *Protanilla* and *P. rafflesi* Taylor (Hymenoptera: Formicidae). *Sociobiology* **59**, 477–491. [Published in 2014] doi:10.13102/sociobiology.v59i2.612

Yamada A, Nguyen DD, Eguchi K (2020) Unveiling the morphology of the Oriental rare monotypic ant genus *Opamyrma* Yamane, Bui & Eguchi, 2008 (Hymenoptera: Formicidae: Leptanillinae) and its evolutionary implications, with first descriptions of the male, larva, tentorium, and sting apparatus. *Myrmecological News* **30**, 27–52. doi:10.25849/myrmecol.news_030:027

Zarei M (2010) Hydrogeology of salt diapirs in the south of Iran. PhD dissertation, Shiraz University, Shiraz, Iran.

**Data availability.** Configuration files, DNA alignment and output for all phylogenetic analyses employed in this study are available on Zenodo (doi:10.5281/zenodo.5595290). Accession numbers for raw UCE reads, uploaded to the Sequence Read Archive (SRA) (https://www.ncbi.nlm.nih.gov/sra), are provided in Table 1.

**Conflicts of interest.** The authors declare that they have no conflicts of interest.

**Declaration of funding.** This research was supported by the UC Davis Department of Entomology, UC Davis Jastro-Shields, and by NSF grant DEB-1932405 to P. S. Ward.

**Acknowledgements.** We thank La Venta Esplorazioni Geografiche for the organiation and funding of the Iran Salt Cave 2019 expedition that led to the discovery of *Y. laventa*. Without La Venta, this species would have remained unknown and the three of us would have never collaborated. The expedition was led by Luca Imperio and Giuseppe Giovine, with the support of Younes Samaridati, our invaluable local guide and interpreter. We thank the Iranian Cave and Speleology Association and the Iran Mountaineering and Sport Climbing Federation (Firuz Abad office) for local support in organising the expedition. Special thanks go to Alessandro Uggeri for providing the geological description of the MSS sites. The second expedition (2020) to collect the traps was assisted by colleagues of M. Moradmand at the University of Isfahan and Yasouj University: Ali Mansouri, Alireza Ghahremani, Behzad Fathinia and Hamid Shahzeidi, for which we are thankful. We thank Jason Bond, Josh Gibson and Charles Stephens for conceptual advice on this project; Michael Branstetter for assembling raw UCE reads; Phil Ward and Ziv Lieberman for writing advice; and Chris Darling (ROME), Brian Fisher (CASC), José María Gómez-Durán, Benoit Guénard (HKUBM), Yu Hisasue, Po-Wei Hsu (NCUE), Debbie Jennings (ANIC), Crystal Maier (MCZC), Jadranka Rota (MZLU), Alberto Tinaut, Kevin Williams (CSCA) and Masashi Yoshimura (OIST) for loans of material used in this study. We also thank Bui Tuan Viet, Katsuyuki Eguchi, Michael Ohl, Christian Rabeling and Michael Sharkey for material sequenced by Borowiec *et al.* (2019) that was also included in this study.

**Author affiliations**

[A]Department of Entomology and Nematology, University of California, Davis, CA, USA.

[B]Laboratorio di Ecologia, Ecosistemi terrestri, Dipartimento di Scienze della Vita e Biologia dei Sistemi, Università di Torino, Torino, Italy.

[C]Department of Plant and Animal Biology, Faculty of Biological Science and Technology, University of Isfahan, Isfahan, Iran.